



Bromine atom production and chain propagation during springtime Arctic ozone depletion events in Barrow, Alaska

Chelsea R. Thompson^{1,a,b}, Paul B. Shepson^{1,2}, Jin Liao^{3,c,d}, L. Greg Huey³, Chris Cantrell^{4,e}, Frank Flocke⁴, and John Orlando⁴

¹Department of Chemistry, Purdue University, West Lafayette, IN, USA

²Department of Earth and Atmospheric Sciences and Purdue Climate Change Research Center, Purdue University, West Lafayette, IN, USA

³School of Earth and Atmospheric Sciences, Georgia Institute of Technology, Atlanta, GA, USA

⁴National Center for Atmospheric Research, Boulder, CO, USA

^anow at: Cooperative Institute for Research in Environmental Sciences, University of Colorado Boulder, Boulder, CO, USA

^bnow at: Chemical Sciences Division, NOAA Earth System Research Laboratory, Boulder, CO, USA

^cnow at: Atmospheric Chemistry and Dynamics Laboratory, NASA Goddard Space Flight Center, Greenbelt, MD, USA

^dnow at: Universities Space Research Association, Columbia, MD, USA

^enow at: Department of Atmospheric and Ocean Sciences, University of Colorado Boulder, Boulder, CO, USA

Correspondence to: Chelsea R. Thompson (chelsea.thompson@noaa.gov)

Received: 22 December 2015 – Discussion started: 18 January 2016

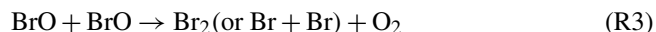
Revised: 1 November 2016 – Accepted: 9 February 2017 – Published: 9 March 2017

Abstract. Ozone depletion events (ODEs) in the Arctic are primarily controlled by a bromine radical-catalyzed destruction mechanism that depends on the efficient production and recycling of Br atoms. Numerous laboratory and modeling studies have suggested the importance of heterogeneous recycling of Br through HOBr reaction with bromide on saline surfaces. On the other hand, the gas-phase regeneration of bromine atoms through BrO–BrO radical reactions has been assumed to be an efficient, if not dominant, pathway for Br reformation and thus ozone destruction. Indeed, it has been estimated that the rate of ozone depletion is approximately equal to twice the rate of the BrO self-reaction. Here, we use a zero-dimensional, photochemical model, largely constrained to observations of stable atmospheric species from the 2009 Ocean–Atmosphere–Sea Ice–Snowpack (OASIS) campaign in Barrow, Alaska, to investigate gas-phase bromine radical propagation and recycling mechanisms of bromine atoms for a 7-day period during late March. This work is a continuation of that presented in Thompson et al. (2015) and utilizes the same model construct. Here, we use the gas-phase radical chain length as a metric for objectively quantifying the efficiency of gas-phase recycling of bromine atoms. The gas-phase bromine chain length is de-

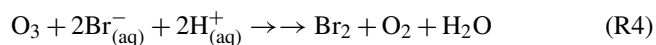
termined to be quite small, at < 1.5 , and highly dependent on ambient O₃ concentrations. Furthermore, we find that Br atom production from photolysis of Br₂ and BrCl, which is predominately emitted from snow and/or aerosol surfaces, can account for between 30 and 90 % of total Br atom production. This analysis suggests that condensed-phase production of bromine is at least as important as, and at times greater than, gas-phase recycling for the occurrence of Arctic ODEs. Therefore, the rate of the BrO self-reaction is not a sufficient estimate for the rate of O₃ depletion.

1 Introduction

The springtime depletion of boundary layer ozone in the Arctic has been the subject of intense research for several decades. Early observations revealed a strong correlation between ozone depletion events (ODEs) and enhancements in filterable bromine (Barrie et al., 1988). This discovery led researchers to propose a mechanism for the bromine-catalyzed destruction of ozone.

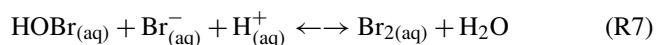


This reaction cycle requires an initial source of bromine atoms to the boundary layer. Laboratory and theoretical studies have suggested that Br_2 could be produced through oxidation of bromide present in salt-enriched snow, ice, or aerosol surfaces by gas-phase ozone (Hirokawa et al., 1998; Oum et al., 1998b; Gladich et al., 2015).



Field observations by Pratt et al. (2013) using a controlled snow chamber experiment with natural tundra snow collected near Barrow, AK, lend further evidence to this mechanism, and also suggest Br_2 production from OH produced photochemically within the snowpack. This mechanism was further explored in the modeling study of Toyota et al. (2014), which suggested an important role for this activation pathway in producing bromine within the snowpack interstitial air.

Once present in the gas-phase, bromine atoms can be regenerated through radical–radical reactions of BrO with XO (where $X = \text{Br}, \text{Cl},$ or iodine: I), NO, OH, or CH_3OO to propagate the chain reaction and continue the destruction cycle of ozone. If BrO photolyzes or reacts with NO, O_3 is regenerated, and there is a null cycle with respect to O_3 . However, although O_3 is not destroyed, these two pathways represent efficient routes for Br atom propagation. Thus, Reaction (R3) serves to make Reaction (R2) effective in destruction of O_3 . At the same time, Br atoms could be recycled through heterogeneous reactions of HOBr with bromide in the condensed phase to release Br_2 to the gas-phase via the now well-known “bromine explosion” mechanism (Vogt et al., 1996; Tang and McConnell, 1996; Fan and Jacob, 1992).



Evidence for reaction sequence (R5)–(R8) has been provided through laboratory studies, which found that Br_2 was produced when frozen bromide solutions were exposed to gas-phase HOBr (Huff and Abbatt, 2002; Adams et al., 2002). This mechanism is believed to proceed rapidly to produce Br_2 so long as sufficient bromide is present in an accessible condensed phase. The efficiency of this heterogeneous recycling mechanism has also been found to have a dependence on the acidity of the surface, as was shown using natural environmental snow samples in Pratt et al. (2013) and investigated in the modeling studies of Toyota et al. (2011, 2014),

in a manner that is consistent with the stoichiometry of Reaction (R7).

To efficiently sustain the ozone destruction cycle to the point of near-complete loss of boundary layer ozone ($[\text{O}_3] < 2$ ppb), bromine atoms must be continually recycled through some combination of the above mechanisms. The gas-phase reaction cycle described by Reactions (R1)–(R3) has generally been considered to be the dominant pathway for Br reformation following the initial activation of Br_2 from the surface (the mechanism for which is still not fully understood). Thus, it has been assumed that the rate of ozone destruction can be estimated as Eq. (1) (see Eq. 15 in Hausmann and Platt, 1994, Eq. 3 in Le Bras and Platt, 1995, and Eq. 7 in Zeng et al., 2006) or as Eq. (2), if chlorine chemistry is considered through Reaction (R9) (Eq. IX in Platt and Janssen, 1995).

$$\frac{d[\text{O}_3]}{dt} = 2 \cdot k_3 \cdot [\text{BrO}]^2 \quad (1)$$

$$\frac{d[\text{O}_3]}{dt} = 2 \left(k_3 \cdot [\text{BrO}]^2 + k_9 \cdot [\text{BrO}] \cdot [\text{ClO}] \right) \quad (2)$$



However, these approximations assume that the ozone destruction rate is dominated by the $\text{BrO} + \text{XO}$ reaction, which in turn necessitates efficient gas-phase recycling of Br; therefore, a relatively long bromine chain length would be required to account for observed rates of ozone destruction. It is, however, possible that Br atoms are generated mostly by Br_2 photolysis, followed by BrO termination, e.g., by Reaction (R5), in which case a short gas-phase bromine radical chain length would be implied. The chain length for any process depends on the rates of the propagation relative to the production and destruction reactions (Kuo, 1986). It is important to note that, in our definition, the chain length refers to radical propagation reactions occurring solely in the gas phase, and is a quantity completely independent of any condensed-phase chemistry. In the stratosphere, the Br–BrO catalytic cycle can have a chain length ranging from 10^2 to 10^4 (Lary, 1996). In the troposphere, there is significantly less solar radiation and many more available sinks; thus, radical chain lengths can be much shorter. For example, the chain length of the tropospheric HO_x cycle has been estimated to be ~ 4 – 5 (Ehhalt, 1999; Monks, 2005), increasing to 10 – 20 near the tropopause (Wennberg et al., 1998). The halogen radical chain lengths in the Arctic troposphere have so far not been determined; thus, it is difficult to evaluate whether Eqs. (1) and (2) are appropriate for estimating ozone depletion rates.

The importance of heterogeneous reactions for recycling reactive bromine has been demonstrated in the recent literature (see review by Abbatt et al., 2012). Modeling studies using typical Arctic springtime conditions to simulate ODEs have concluded that ozone depletion cannot be sustained

without considering the heterogeneous recycling of reactive bromine on snow or aerosol surfaces (e.g., Michalowski et al., 2000; Piot and Von Glasow, 2008; Liao et al., 2012b; Toyota et al., 2014). Michalowski et al. (2000) determined that the rate of ozone depletion in their model was limited by the mass transfer rate of HOBr to the snowpack (effectively, the rate at which Br is recycled through the heterogeneous mechanism) and that the depletion of ozone is nearly completely shut down when snowpack interactions are removed. Piot and von Glasow (2008) simulated ozone depletion using the one-dimensional MISTRA model and concluded that major ODEs (defined as complete destruction within 4 days) could only be produced if recycling of deposited bromine on snow is included. Without heterogeneous recycling on the snowpack, the BrO_x termination steps and irreversible loss of HOBr and HBr to the surface prohibits the occurrence of an ODE. More recently, using HOBr observations from Barrow during OASIS (Ocean–Atmosphere–Sea Ice–Snowpack) study, Liao et al. (2012b) found that a simple photochemical model overpredicted observed HOBr during higher wind events ($> 6 \text{ m s}^{-1}$), ostensibly due to an underpredicted heterogeneous loss to aerosol in the model, and concluded that their field observations support the hypothesis of efficient recycling back to reactive bromine via this mechanism.

It is evident that the reactions occurring on snow and aerosol surfaces are likely the initial source of halogen species to the polar boundary layer and that heterogeneous bromine recycling on these surfaces must be considered for HOBr and HBr (as well as BrNO_2 and BrONO_2 in higher NO_x environments). However, the relative importance of gas-phase recycling of bromine atoms is uncertain, even though it is often assumed that the ozone depletion rate can be estimated reasonably well by the catalytic gas-phase radical reaction rates. The goal of this work was to investigate gas-phase Br atom propagation in terms of the bromine chain length in comparison to the production of Br atoms through photolysis of Br_2 and BrCl , which are predominantly produced directly from surface emissions and/or aerosol release. Here, we present results from our study using a zero-dimensional model constrained with time-varying measurements of molecular halogens, HOBr, O_3 , CO, NO, NO_2 , and VOCs (volatile organic compounds) from the 2009 OASIS campaign in Barrow, Alaska. This work builds on the analysis presented in Thompson et al. (2015) using the same model framework. By constraining our model with observations, we were able to conduct an in-depth study of the halogen atom recycling occurring under varying conditions that were observed during the campaign.

2 Experimental

2.1 Measurements and site description

The analysis presented herein utilizes observations conducted during the OASIS field campaign that occurred during the months of February through April of 2009 in Barrow, AK. The goal of the OASIS study was to investigate the chemical and physical processes occurring within the surface boundary layer during ozone and mercury depletion events in polar spring. This study resulted in the largest suite of simultaneous and co-located atmospheric measurements conducted in the Arctic near-surface atmosphere to date, and represents a unique opportunity for in-depth examination of a multitude of chemical interactions in this environment.

Atmospheric measurements were conducted from instrument trailers located near the Barrow Arctic Research Consortium (BARC) facility on the Naval Arctic Research Laboratory (NARL) campus. Winds arriving at the site are primarily northeasterly, from over the sea ice, and thus represent background conditions with influence from natural processes and snow–air interactions. Winds occasionally shift to westerly, bringing local emissions from the town of Barrow to the site; however, these isolated events are easily identifiable by coincident enhancements in both NO_x and CO.

Measurements of molecular halogens, HOBr, NO, NO_2 , O_3 , CO, and VOCs were used to constrain the model employed in this analysis. Instrumental methods for these measurements have all been described elsewhere; thus, only a brief description is provided here. Inorganic halogen species (Br_2 , Cl_2 , BrO, and HOBr) were measured by chemical ionization mass spectrometry with I^- ion chemistry as described in Liao et al. (2011, 2012b, 2014); O_3 , NO, and NO_2 were measured by chemiluminescence (Ridley et al., 1992; Ryerson et al., 2000). CO was measured using a standard commercial CO analyzer (Thermo Scientific) with infrared absorption detection, and formaldehyde (HCHO) was measured at 1 Hz frequency using a tunable diode laser absorption spectrometer, as described in Fried et al. (1997) and Lancaster et al. (2000). A large suite of organic compounds was measured in situ by fast GC-MS (Apel et al. 2010) and via whole air canister samples with offline GC-MS (Russo et al., 2010).

2.2 Model description

The model used for this study is a zero-dimensional box model developed using the commercial software FACSIMILE. A detailed description of the model can be found in Thompson et al. (2015). We will describe the model only briefly here.

Our model consists of 220 gas-phase reactions and 42 photolysis reactions, representing much of the known gas-phase chemistry occurring in the Arctic, including the important halogen, HO_x , NO_x , and VOC chemistry associated with ozone depletions. The model also includes an inor-

ganic iodine reaction scheme adapted from McFiggans et al. (2000, 2002), Calvert and Lindberg (2004), and Saiz-Lopez et al. (2008). Although IO has not been unambiguously measured in the High Arctic above the $\sim 1.5\text{--}2$ pptv detection limit of LP-DOAS (long-path differential optical absorption spectroscopy), observed enhancements in filterable iodide and total iodine suggest that iodine chemistry is active to some extent in this region (Sturges and Barrie, 1988; Martinez et al., 1999; Mahajan et al., 2010; Hönninger, 2002). Recently, I_2 has been detected at tens of pptv within the snowpack interstitial air near Barrow, AK, and at ≤ 0.5 pptv in the near surface air by I^- chemical ionization mass spectrometry (CIMS), providing direct evidence supporting the presence of at least low levels of iodine chemistry (Raso et al., 2017). In our previous study (Thompson et al., 2015), we investigated the impact of two different hypothetical levels of iodine. Here, we investigate only the “low iodine” scenario for certain calculations, in which a diurnally varying I_2 flux is incorporated such that average daytime mixing ratios of IO remain near 1 pptv for the majority of the simulation. These levels of IO are realistic given our current knowledge based on the work of Hönninger (2002) and Raso et al. (2017).

All gas-phase rate constants used in this model were calculated for a temperature of 248 K, consistent with average daytime conditions in Barrow for the period simulated. Although some gas-phase reactions can exhibit a significant temperature dependence, we chose not to incorporate variable temperatures into our model. This is justified in this case because ambient temperature in Barrow for the week of 25 March 2009 varied by less than 10 K between the maximum and minimum recorded daily temperatures. The radical oxidation and radical–radical reactions that are of primary importance here do not have a large temperature dependence (Atkinson et al., 2006, 2007); for example, a variability of 10 K imposes an $\sim 1\%$ change on the rate of ethane oxidation by Cl atoms and a $< 4\%$ change on the rate of the $\text{BrO} + \text{BrO}$ radical self-reaction. Most radical–radical reactions have only a small negative-temperature dependence. Furthermore, and as mentioned previously, the major non-radical chemical species driving the model are highly constrained to observations and are not allowed to freely evolve. Table 1 contains an abbreviated list of the reactions included in the model, showing only those reactions that are central to the production, propagation, and termination of bromine radical chemistry, which is the focus of this study. A complete list of reactions can be found in Thompson et al. (2015).

The model is configured to simulate 7 days during late March, 25 through 31 March, that include a period of depleting ozone, a full ozone depletion ($[\text{O}_3] < 2$ ppbv) lasting for ~ 3 days, and recovery. The O_3 time series for this period is shown in Fig. 1a, along with radiation as a reference (all plots are in Alaska standard time). We constrain the model to observations for this time period by reading in time-varying data sets of O_3 , C_2H_2 , C_2H_4 , C_2H_6 , C_3H_8 , C_3H_6 , $n\text{-C}_4\text{H}_{10}$,

$i\text{-C}_4\text{H}_{10}$, HCHO, CH_3CHO , CH_3COCH_3 , methyl ethyl ketone (MEK), Cl_2 , Br_2 , HOBr, NO, NO_2 , and CO at 10 min time steps. All other gas-phase species are allowed to freely evolve. Surface fluxes (represented as volumetric fluxes) are used for HONO and I_2 and are scaled to $J(\text{NO}_2)$ as a proxy for radiation as both of these species are likely to be produced photochemically. Further discussion regarding HONO can be found in Thompson et al. (2015).

Photolysis rate constants (J coefficients) for many of the species included were calculated during OASIS using the Tropospheric Ultraviolet and Visible Radiation model from measurements of down-welling actinic flux conducted throughout the campaign (Shetter and Müller, 1999; Stephens et al., 2012). Estimates of J_{max} in the Arctic for OCIO were taken from Pöhler et al. (2010), for HOCl from Lehrer et al. (2004), and for CHBr_3 from Papanastasiou et al. (2014). J_{max} values for the iodine compounds were calculated according to the work of Calvert and Lindberg (2004), which also simulated conditions for late March in Barrow, Alaska. Time-varying J coefficients for O_3 and NO_2 were read into the model at 10 min time steps. All other photolysis reactions were scaled to $J(\text{NO}_2)$ in the modeling code using the maximum J coefficients (J_{max}) for 25 March (a clear-sky day) as a basis for scaling. For cloudy days, this method assumes that J coefficients for other photolytically active species are attenuated in a manner that is proportional to $J(\text{NO}_2)$.

In the initial development of the model, heterogeneous reactions of halogen species occurring on aerosol and snowpack surfaces were included, as well as mass transfer and dry deposition for certain species using the method and mechanism of Michalowksi et al. (2000). This mechanism assumes aqueous-phase kinetics for those reactions occurring within a uniformly distributed quasi-liquid layer (QLL), in a similar fashion as numerous other models (e.g., Piot and von Glasow, 2008; Thomas et al., 2011; Toyota et al., 2014). It was originally intended to utilize this multiphase chemistry to produce halogen radical precursors. However, the heterogeneous production mechanisms could not reproduce observed Br_2 or Cl_2 from OASIS. This reflects the complex but not fully understood condensed-phase chemistry and physics that lead to the production of Br_2 (and Cl_2) (Abbatt et al., 2012; Domine et al., 2013; Pratt et al., 2013). Additionally, the current knowledge of the physical properties of the QLL and the location of liquid-like surfaces on snow grains would seem to invalidate the aforementioned assumptions on which many of the current heterogeneous models are based (Domine et al., 2013), specifically that the chemistry occurs in a liquid-like environment on snow grains. Indeed, Cao et al. (2014) adopted a simplified heterogeneous chemistry mechanism in their modeling of Arctic ozone depletion, wherein they use the mass transfer of HOBr to the surface as the rate-limiting step in Br_2 production, citing the lack of suitable reaction mechanisms with which to properly simulate condensed-phase chemistry on snow/ice. Ad-

Table 1. Reactions used in the model that are pertinent to bromine chemistry. All rate constants (with the exception of photolysis J coefficients) are in units of $\text{cm}^3 \text{ molecule}^{-1} \text{ s}^{-1}$.

Gas-phase reactions	Rate constant	Reference	
$\text{Br} + \text{O}_3 \rightarrow \text{BrO}$	6.75×10^{-13}	Atkinson et al. (2004)	
$\text{Br} + \text{C}_2\text{H}_4 \rightarrow \text{HBr} + \text{C}_2\text{H}_5\text{OO}$	1.3×10^{-13}	Atkinson et al. (2004)	
$\text{Br} + \text{C}_3\text{H}_6 \rightarrow \text{HBr} + \text{C}_3\text{H}_5$	1.60×10^{-12}	Atkinson et al. (2004)	
$\text{Br} + \text{HCHO} \rightarrow \text{HBr} + \text{CO} + \text{HO}_2$	6.75×10^{-13}	Sander et al. (2006)	
$\text{Br} + \text{CH}_3\text{CHO} \rightarrow \text{HBr} + \text{CH}_3\text{COOO}$	2.8×10^{-12}	Atkinson et al. (2004)	
$\text{Br} + \text{C}_3\text{H}_6\text{O} \rightarrow \text{HBr}$	9.7×10^{-12}	Wallington et al. (1989)	
$\text{Br} + \text{nButanal} \rightarrow \text{HBr}$	9.7×10^{-12}	estimate from Michalowski et al. (2000)	
$\text{Br} + \text{CH}_3\text{OOH} \rightarrow \text{HBr} + \text{CH}_3\text{OO}$	4.03×10^{-15}	Mallard et al. (1993)	
$\text{Br} + \text{NO}_2 \rightarrow \text{BrNO}_2$	2.7×10^{-11}	Atkinson et al. (1993)	
$\text{Br} + \text{BrNO}_3 \rightarrow \text{Br}_2 + \text{NO}_3$	4.9×10^{-11}	Orlando and Tyndall (1996)	
$\text{Br} + \text{OCIO} \rightarrow \text{BrO} + \text{ClO}$	1.43×10^{-13}	Atkinson et al. (2004)	
$\text{BrO} + \text{O}(^3\text{P}) \rightarrow \text{Br}$	4.8×10^{-11}	Atkinson et al. (2004)	
$\text{BrO} + \text{OH} \rightarrow \text{Br} + \text{HO}_2$	4.93×10^{-11}	Atkinson et al. (2004)	
$\text{BrO} + \text{HO}_2 \rightarrow \text{HOBr}$	3.38×10^{-11}	Atkinson et al. (2004)	
$\text{BrO} + \text{CH}_3\text{OO} \rightarrow \text{HOBr} + \text{CH}_2\text{OO}$	4.1×10^{-12}	Aranda et al. (1997)	
$\text{BrO} + \text{CH}_3\text{OO} \rightarrow \text{Br} + \text{HCHO} + \text{HO}_2$	1.6×10^{-12}	Aranda et al. (1997)	
$\text{BrO} + \text{CH}_3\text{COOO} \rightarrow \text{Br} + \text{CH}_3\text{COO}$	1.7×10^{-12}	estimate from Michalowski et al. (2000)	
$\text{BrO} + \text{C}_3\text{H}_6\text{O} \rightarrow \text{HOBr}$	1.5×10^{-14}	estimate from Michalowski et al. (2000)	
$\text{BrO} + \text{NO} \rightarrow \text{Br} + \text{NO}_2$	2.48×10^{-11}	Atkinson et al. (2004)	
$\text{BrO} + \text{NO}_2 \rightarrow \text{BrNO}_3$	1.53×10^{-11}	Atkinson et al. (2004)	
$\text{BrO} + \text{BrO} \rightarrow \text{Br} + \text{Br}$	2.82×10^{-12}	Sander et al. (2006)	
$\text{BrO} + \text{BrO} \rightarrow \text{Br}_2$	9.3×10^{-13}	Sander et al. (2006)	
$\text{BrO} + \text{HBr} \rightarrow \text{HOBr} + \text{Br}$	2.1×10^{-14}	Hansen et al. (1999)	
$\text{HBr} + \text{OH} \rightarrow \text{Br} + \text{H}_2\text{O}$	1.26×10^{-11}	Sander et al. (2006)	
$\text{CH}_3\text{Br} + \text{OH} \rightarrow \text{H}_2\text{O} + \text{Br}$	1.27×10^{-14}	Atkinson et al. (2004)	
$\text{CHBr}_3 + \text{OH} \rightarrow \text{H}_2\text{O} + \text{Br}$	1.2×10^{-13}	Atkinson et al. (2004)	
$\text{Cl} + \text{BrCl} \rightleftharpoons \text{Br} + \text{Cl}_2$	$f: 1.5 \times 10^{-11} \quad r: 1.1 \times 10^{-15}$	Clyne et al. (1972)	
$\text{Cl} + \text{Br}_2 \rightleftharpoons \text{BrCl} + \text{Br}$	$f: 1.2 \times 10^{-10} \quad r: 3.3 \times 10^{-15}$	Clyne et al. (1972)	
$\text{BrO} + \text{ClO} \rightarrow \text{Br} + \text{Cl}$	7.04×10^{-12}	Atkinson et al. (2004)	
$\text{BrO} + \text{ClO} \rightarrow \text{BrCl}$	1.15×10^{-12}	Atkinson et al. (2004)	
$\text{BrO} + \text{ClO} \rightarrow \text{Br} + \text{OCIO}$	9.06×10^{-12}	Atkinson et al. (2004)	
$\text{HOBr} + \text{OH} \rightarrow \text{BrO} + \text{H}_2\text{O}$	5.0×10^{-13}	Kukui et al. (1996)	
$\text{HOBr} + \text{Cl} \rightarrow \text{BrCl} + \text{OH}$	8.0×10^{-11}	Kukui et al. (1996)	
$\text{HOBr} + \text{O}(^3\text{P}) \rightarrow \text{BrO} + \text{OH}$	2.12×10^{-11}	Atkinson et al. (2004)	
$\text{IO} + \text{BrO} \rightarrow \text{Br} + \text{OIO}$	9.36×10^{-11}	Atkinson et al. (2004)	
$\text{IO} + \text{BrO} \rightarrow \text{IBr}$	4.32×10^{-11}	Atkinson et al. (2004)	
$\text{IO} + \text{BrO} \rightarrow \text{Br} + \text{I}$	7.2×10^{-12}	Atkinson et al. (2004)	
Photolysis reactions	J_{max} (25 March) s^{-1}	Lifetime	Reference
$\text{BrNO}_3 \rightarrow \text{Br} + \text{NO}_3$	2.1×10^{-4}	1.3 h	calculated from OASIS data
$\text{BrNO}_3 \rightarrow \text{BrO} + \text{NO}_2$	1.2×10^{-3}	14.2 min	calculated from OASIS data
$\text{BrO} \rightarrow \text{Br} + \text{O}(^3\text{P})$	3.0×10^{-2}	33 s	calculated from OASIS data
$\text{Br}_2 \rightarrow \text{Br} + \text{Br}$	4.4×10^{-2}	23 s	calculated from OASIS data
$\text{HOBr} \rightarrow \text{Br} + \text{OH}$	2.3×10^{-3}	7.2 min	calculated from OASIS data
$\text{BrNO}_2 \rightarrow \text{Br} + \text{NO}_2$	1.5×10^{-4}	1.8 h	estimate from Lehrer et al. (2004)
$\text{BrCl} \rightarrow \text{Br} + \text{Cl}$	1.26×10^{-2}	1.3 min	calculated from OASIS data

Table 1. Continued.

Mass transfer reactions	k_t (forward)	k_t (reverse)	
$\text{HBr}_{(\text{g})} \rightarrow \text{H}_{(\text{p})}^+ + \text{Br}_{(\text{p})}^-$	1.80×10^{-3}		
$\text{HCl}_{(\text{g})} \rightarrow \text{H}_{(\text{p})}^+ + \text{Cl}_{(\text{p})}^-$	2.58×10^{-3}		
$\text{HOBr}_{(\text{g})} \rightarrow \text{HOBr}_{(\text{p})}$	1.26×10^{-3}		
$\text{BrNO}_{2(\text{g})} \rightarrow \text{BrNO}_{2(\text{p})}$	1.26×10^{-3}		
$\text{BrONO}_{3(\text{g})} \rightarrow \text{BrONO}_{3(\text{p})}$	1.26×10^{-3}		
$\text{Br}_{2(\text{g})} \leftrightarrow \text{Br}_{2(\text{p})}$	1.78×10^{-5}	2.97×10^8	
$\text{BrCl}_{(\text{g})} \leftrightarrow \text{BrCl}_{(\text{p})}$	6.60×10^{-4}	1.91×10^{10}	
$\text{IBr}_{(\text{p})} \rightarrow \text{IBr}_{(\text{g})}$	5.53×10^9		
$\text{HBr}_{(\text{g})} \rightarrow \text{H}_{(\text{s})}^+ + \text{Br}_{(\text{s})}^-$	1.67×10^{-5}		
$\text{HCl}_{(\text{g})} \rightarrow \text{H}_{(\text{s})}^+ + \text{Cl}_{(\text{s})}^-$	1.67×10^{-5}		
$\text{HOBr}_{(\text{g})} \rightarrow \text{HOBr}_{(\text{s})}$	1.67×10^{-5}		
$\text{BrNO}_{2(\text{g})} \rightarrow \text{BrNO}_{2(\text{s})}$	1.67×10^{-4}		
$\text{BrONO}_{3(\text{g})} \rightarrow \text{BrONO}_{3(\text{s})}$	1.26×10^{-4}		
$\text{Br}_{2(\text{g})} \leftrightarrow \text{Br}_{2(\text{s})}$	1.0×10^{-5}	7.71×10^{-2}	
$\text{BrCl}_{(\text{g})} \leftrightarrow \text{BrCl}_{(\text{s})}$	1.25×10^{-5}	7.71×10^{-2}	
$\text{IBr}_{(\text{s})} \rightarrow \text{IBr}_{(\text{g})}$	7.71×10^{-2}		
Aqueous-phase reactions	k (particle)	k (snow)	Reference
$\text{Cl}^- + \text{HOBr} + \text{H}^+ \rightarrow \text{BrCl}$	5.17×10^{-21}	9.30×10^{-26}	Wang et al. (1994)
$\text{Br}^- + \text{HOCl} + \text{H}^+ \rightarrow \text{BrCl}$	1.2×10^{-24}	2.15×10^{-29}	Sander et al. (1997)
$\text{Br}^- + \text{HOBr} + \text{H}^+ \rightarrow \text{Br}_2$	1.47×10^{-20}	2.64×10^{-25}	Beckwith et al. (1996)
$\text{Br}^- + \text{HOI} + \text{H}^+ \rightarrow \text{IBr}$	3.04×10^{-18}	5.46×10^{-23}	Troy et al. (1991)
$\text{BrCl} + \text{Cl}^- \rightarrow \text{BrCl}_2^-$	3.3	5.99×10^{-5}	Michalowski et al. (2000)
$\text{BrCl}_2^- \rightarrow \text{BrCl} + \text{Cl}^-$	1.58×10^9	1.58×10^9	Michalowski et al. (2000)
$\text{BrCl} + \text{Br}^- \rightarrow \text{Br}_2\text{Cl}^-$	3.3	5.99×10^{-5}	Michalowski et al. (2000)
$\text{Br}_2\text{Cl}^- \rightarrow \text{BrCl} + \text{Br}^-$	3.34×10^5	3.34×10^5	Wang et al. (1994)
$\text{Cl}_2 + \text{Br}^- \rightarrow \text{BrCl}_2^-$	4.27	7.66×10^{-5}	Wang et al. (1994)
$\text{BrCl}_2^- \rightarrow \text{Cl}_2 + \text{Br}^-$	6.94×10^2	6.94×10^2	Wang et al. (1994)
$\text{O}_3 + \text{Br}^- \rightarrow \text{HOBr}$	4.5×10^{-9}	8.08×10^{-14}	Oum et al. (1998)

mitedly, our model is also not able to capture these complex heterogeneous processes. However, as discussed thoroughly by Domine et al. (2013), even our most complex state-of-the-art snow chemistry models are neither physically nor chemically accurate, and rely upon a variety of adjustable parameters to produce reasonable results, because of the lack of fundamental understanding of the actual phase and physical and chemical environment in which the chemistry is occurring. It is thus clear that the kinetics of the individual reactions in such a case cannot be reliably simulated.

In light of the limitations of all models of cryosphere photochemistry, a strength of this study, and opportunity, rests with the fact that we have observations of key halogen species, including Br_2 , Cl_2 , BrO , ClO , HOBr , as well as VOCs, NO_x , OH , and HO_2 . Therefore, to study the gas-phase recycling discussed in the Introduction, in this work Br_2 and Cl_2 concentrations were fixed at the observed levels (see Thompson et al., 2015, for further discussion) and were not produced via heterogeneous chemistry. During a period spanning a portion of 29 and 30 March, Br_2 observa-

tions are not available due to instrument instability. Here, we have filled in the missing portion of data with average daytime Br_2 values based on observations from 27 and 28 March and the morning data available for 29 March, and use average nighttime values for the night of 29/30 March using the observations from the two adjacent nighttime periods. The filled-in values for Br_2 result in reasonable agreement between modeled and observed BrO for this period. In the analyses presented in Figs. 3 and 5–10 we have indicated this period of missing and filled-in Br_2 values with a shaded box. Due to the sparseness of BrCl observations during OASIS, only daytime BrCl was used as produced in the model multiphase mechanism. While we do not argue that the production mechanism for BrCl is accurate, the daytime simulated BrCl mixing ratios of 0–10 pptv are in approximate agreement with the available data for the campaign. In any case, according to our model, BrCl was not a significant source of either Br or Cl atoms relative to Br_2 and Cl_2 .

Though we do not use the heterogeneous chemistry module for any chemical production (other than BrCl), deposi-

tion and mass transfer is a significant and critical sink for certain species. Thus, we do make use of this aspect of the multiphase portion of the model, as described below. The dry deposition velocity of O_3 to the snowpack is estimated at 0.05 cm s^{-1} , consistent with previous measurements and modeling studies (Gong et al., 1997; Michalowski et al., 2000; Helmig et al., 2007; Cavender et al., 2008), though it is recognized that there is large uncertainty with this parameter from field observations (Helmig et al., 2007, 2012). Assuming a boundary layer height of 300 m, this corresponds to a transfer coefficient, k_t , of $1.67 \times 10^{-6} \text{ s}^{-1}$. Though we have incorporated the deposition of O_3 in the model, the *gas-phase* mixing ratio of O_3 is constrained to observations, which adjusts on 10 min time steps. Dry deposition velocities for the stable Arctic environment have not been determined for the halogen acids (HBr, HCl, HOBr, HOCl, HOI); therefore, we use the estimation method of Michalowski et al. (2000) and assume a deposition velocity that is 10 times greater than for O_3 , leading to a k_t of $1.67 \times 10^{-5} \text{ s}^{-1}$. In most model runs, we have chosen to constrain to HOBr observations (further described in Sect. 3.1), and thus a similar situation exists as for O_3 mentioned above. We assume an equivalent k_t for the oxidized nitrogen compounds (HNO_3 , HO_2NO_2 , HONO, N_2O_5 , $BrNO_2$, and $BrONO_2$). The mass transfer coefficient of atmospheric species to the particle phase is calculated as a first-order process as described in Jacob (2000). The concentration of aerosol surface area used was $3.95 \times 10^{-7} \text{ cm}^2 \text{ cm}^{-3}$ as calculated by Michalowski et al. (2000) from measurements made at Alert by Staebler et al. (1994), with a maximum aerosol radius of $r = 0.1 \mu\text{m}$. These levels are also consistent with observations of aerosol surface area at Barrow, which ranged between 9×10^{-8} and $40 \times 10^{-7} \text{ cm}^2 \text{ cm}^{-3}$ (Liao et al., 2012b). We recognize that this constant level of aerosols imparts a constant loss rate in the model and does not take into account any variability in the uptake strength. Because many of these species are lacking empirically derived deposition velocities (e.g., HOBr), there is necessarily large uncertainty in these values, and it is not possible at this time to ascertain whether the uncertainty associated with the deposition velocity estimation is greater or less than the uncertainty imposed by using a constant aerosol surface area. Liao et al. (2012b) did use time-varying aerosol surface area from observations at Barrow; however, they suggested that simple parameterization of deposition of HOBr to aerosols was insufficient for accurately simulating HOBr (further discussion of HOBr is in Sect. 3.1). Given the highly simplified nature of the surface deposition in our model, we do not attempt to differentiate between aerosol uptake and deposition to the snow surface, and instead we lump these two terms together under the “surface deposition” umbrella. However, while we mostly constrain the model to observed HOBr, the comparison to simulated HOBr using these values is instructive.

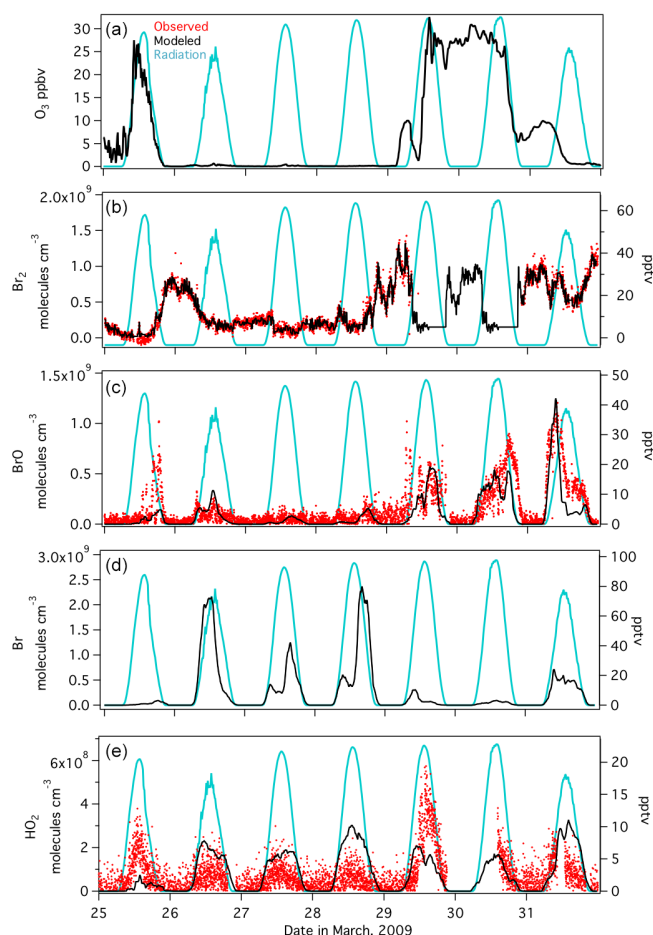


Figure 1. Time series of gas-phase concentrations and mixing ratios of O_3 , Br_2 , BrO , Br , and HO_2 in the model (black trace) for the 7-day period simulated. Observations are plotted in red where available for Br_2 , BrO , and HO_2 . O_3 and Br_2 are constrained species in the model. Simulated output of BrO , Br , and HO_2 are smoothed by hourly averaging. Radiation is shown as the cyan trace as a reference. Time is expressed in Alaska standard time.

3 Results and discussion

3.1 Comparison of modeled and observed Br_2 , BrO , $HOBr$, and HO_2

This work focuses on the propagation and production mechanisms of Br atoms, and thus it is critical that our model accurately captures BrO and Br_2 at mixing ratios that are consistent with observations. Figure 1b and c show comparisons between modeled mixing ratios (black trace) of Br_2 and BrO compared to the measured values during this time (red data) by CIMS (Liao et al., 2012b). Modeled BrO is presented as hourly averages. In the model, Br_2 is fixed to time-varying observations, whereas BrO is produced strictly through the gas-phase photochemical reactions. The model captures the overall temporal profile and magnitude of BrO throughout the period. It should be noted, however, that the uncertainty

in the BrO measurements is large during ODEs as the observed values are very near the limit of detection (LOD of ~ 2 pptv with uncertainty of $-3/+1$ pptv near the LOD).

Br₂ mixing ratios reach 2–12 pptv (Fig. 1b) during the daytime. Given the short lifetime of Br₂ resulting from rapid photolysis, these daytime mixing ratios imply a large surface flux, that in turn produces the BrO mixing ratios observed. These Br₂ levels are consistent with previous Arctic measurements that observed daytime Br₂ up to 27 pptv (Foster et al., 2001) and agree well with the “uncorrected” Br₂ data reported in Liao et al. (2012a, b) for this period. It has been suggested that daytime Br₂ greater than the CIMS instrumental detection limit (~ 1 pptv) is an artifact of HOBr conversion to Br₂ on the instrument using an aircraft inlet (Neuman et al., 2010); however, for the instrument configuration employed during OASIS, it is not clear how much, if any, of the Br₂ signal is a result of HOBr reactions on instrument surfaces.

An estimate of the effective mixing height of Br₂ can be calculated using the method of Guimbaud et al. (2002) and using an average measured diffusivity during OASIS of $1500 \text{ cm}^2 \text{ s}^{-1}$ (R. Staebler, personal communication, 2015). By assuming that photolysis is the dominant loss mechanism controlling the Br₂ midday lifetime in a stable boundary layer typical of Arctic conditions, the daytime effective mixing height is ~ 1.85 m. This also assumes that the snowpack is the primary source of Br₂ emissions, which is consistent with previous assumptions for the aldehydes (Sumner and Shepson, 1999; Guimbaud et al., 2002) and is supported by direct empirical evidence of the tundra snowpack being a relatively strong source of Br₂ (Pratt et al., 2013). Enhanced Br₂ within the snowpack interstitial air has also been predicted from the modeling studies of Toyota et al. (2011, 2014). From this estimation, a significant fraction of the Br₂ present at the surface would remain at the height of the instrument inlet (~ 1 m) in the sunlit periods. If aerosols do represent a significant source of Br₂ as has been hypothesized, and inferred indirectly from bromide depletion in sea salt aerosols (Sander et al., 2003), then one would expect enhanced Br₂ to be present throughout the height of the boundary layer. In our highly constrained model, daytime Br₂ mixing ratios greater than 1 pptv are necessary to reproduce observed BrO; therefore, this modeling study suggests that Br₂ should indeed be present and above the instrument detection limit during the daytime. Br atoms are predicted at concentrations ranging from 1×10^7 to 3×10^9 molecules cm^{-3} . The hourly averaged model output for Br is shown in Fig. 1d. No direct measurements of Br atoms are available with which to compare, though these values are within the range of estimates determined by Jobson et al. (1994) and Ariya et al. (1998).

In the case of HOBr, our model originally simulated this species based on the known gas-phase sources and sinks (including photolysis) and deposition/uptake to surfaces as described above. As shown in Thompson et al. (2015), and again in Fig. 2a, given the observed Br₂ mixing ratios, the

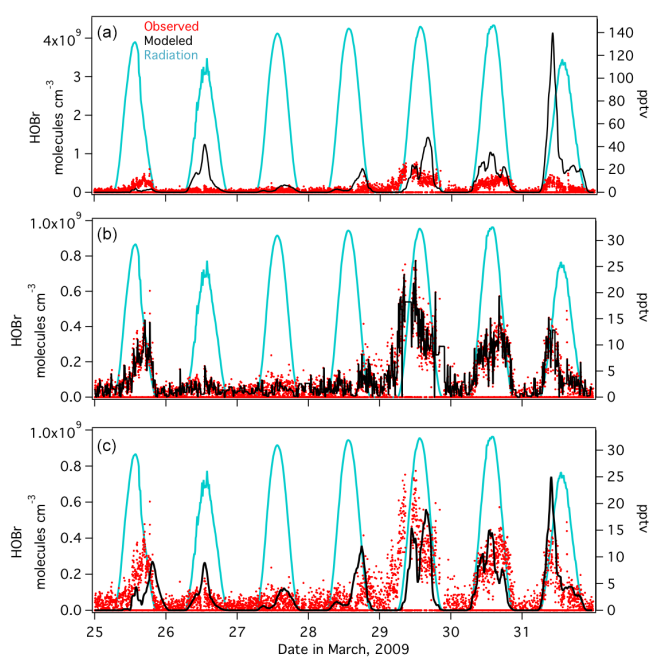


Figure 2. Simulated (black trace) versus observed (red markers) HOBr mixing ratios shown for three different versions of the model: (a) HOBr unconstrained and allowed to freely evolve with a constant surface deposition term as described in the Methods, (b) HOBr constrained to observations, (c) HOBr unconstrained but with a variable surface deposition that is enhanced during higher wind speeds. Simulated (unconstrained) output in (a, c) are smoothed by hourly averaging. Radiation is shown as the cyan trace as a reference. Time is expressed in Alaska standard time.

model greatly overestimated HOBr. Liao et al. (2012b) simulated inorganic bromine species from the OASIS campaign using a simple steady-state model and experienced that their model also overestimated the observed HOBr, with the overestimation becoming especially pronounced during periods of higher winds. They suggested a faster heterogeneous loss to aerosols or blowing snow that was not represented in their model, despite utilizing time-varying aerosol surface area from observations. For the majority of the results presented in this work, we chose to operate our model constrained to HOBr observations, as illustrated in Fig. 2b. Figure 2c shows modeled HOBr obtained by adjusting the deposition to aerosols based on daily wind speeds (resulting in k_t values ranging from 1×10^{-2} to $1.5 \times 10^{-4} \text{ s}^{-1}$), and tuned to provide reasonable agreement with observations. This resulted in smaller deposition rates on 25 through 27 March when winds were calm, and higher deposition rates on 29 through 31 March when winds were up to 9 m s^{-1} . This method allowed us to calculate the importance of surface deposition of HOBr relative to photolysis as a sink for this compound, but the constrained version of the model was used for all other calculations, e.g., for the chain length calculations.

HO₂ is essential for the heterogeneous recycling of bromine (via Reactions R5–R7). Therefore, it is important that our model provides a reasonable estimation of HO₂ for this analysis. In Fig. 1e we show a comparison of simulated, hourly averaged HO₂ (black trace) and observed HO₂ from OASIS for this period (red data), measured using a CIMS developed for peroxy radicals (Edwards et al., 2003). The range of daytime HO₂ mixing ratios is reproduced reasonably well. Simulated HO₂ is on the lower limit of observations for 25 and 29 March, and does not reach the maximum mixing ratios observed. The model also somewhat overpredicts HO₂ on 28 through 30 March; however, the model values are within the stated 25–100 % range of uncertainty of the measurement.

3.2 Chain length

The ozone destruction cycle as described in Reactions (R1)–(R3) is a chain reaction mechanism catalyzed by BrO_x. The effectiveness of a catalytic cycle can be quantified by considering the chain length, that is, the number of free radical propagation cycles per termination or per initiation. The radical chain length is a metric that refers solely to gas-phase reactions (Monks, 2005). We have not, until the OASIS 2009 campaign, had the high quality measurements available to enable a reliable estimation of the bromine radical chain length in the Arctic.

The length of the chain in a radical propagation cycle is limited by termination steps that destroy the chain carriers and result in relatively stable atmospheric species. Thus, the chain length can be defined as the rate of propagation divided by the rate of termination. Alternatively, the chain length can also be calculated using the rate of initiation. If the total bromine radical population is at steady state, the rate of initiation is equal to the rate of termination; thus, for short-lived radical species, the two methods for calculating chain length should be approximately equal.

$$\text{Method 1 : } \Phi = \frac{\Sigma(\text{Rates of propagation})}{\Sigma(\text{Rates of termination})} \quad (3)$$

$$\text{Method 2 : } \Phi = \frac{\Sigma(\text{Rates of propagation})}{\Sigma(\text{Rates of initiation})} \quad (4)$$

We used our model to calculate the chain length for bromine radical propagation across the 7 days of the simulated period using both Methods 1 and 2 as shown in Eqs. (5) and (6). Because bromine radicals are generated photolytically, the chain length is calculated for daytime only, defined here as approximately 07:00 to 21:00 Alaska standard time (AKST).

$$\begin{aligned} \text{Method 1 : } \Phi_{\text{Br}} = & \left(2k[\text{BrO}]^2 + J_{\text{BrO}}[\text{BrO}] + k[\text{BrO}][\text{ClO}] \right. \\ & + k[\text{BrO}][\text{IO}] + k[\text{BrO}][\text{CH}_3\text{OO}] \\ & + k[\text{BrO}][\text{OH}] + k[\text{BrO}][\text{O}(\text{}^3\text{P})] \\ & \left. + k[\text{BrO}][\text{CH}_3\text{COOO}] + k[\text{BrO}][\text{NO}] \right) \\ & \left(k[\text{Br}][\text{HO}_2] + k[\text{Br}][\text{C}_2\text{H}_2] + k[\text{Br}][\text{C}_2\text{H}_4] \right. \\ & + k[\text{Br}][\text{C}_3\text{H}_6] + k[\text{Br}][\text{HCHO}] + k[\text{Br}][\text{NO}_2] \\ & + k[\text{Br}][\text{CH}_3\text{CHO}] + k[\text{Br}][\text{C}_3\text{H}_6\text{O}] + k[\text{Br}][\text{C}_4\text{H}_8\text{O}] \\ & + k[\text{Br}][\text{CH}_3\text{OOH}] + k[\text{BrO}][\text{HO}_2] + k[\text{BrO}][\text{CH}_3\text{OO}] \\ & \left. + k[\text{BrO}][\text{C}_3\text{H}_6\text{O}] + k[\text{BrO}][\text{NO}_2] \right) \quad (5) \end{aligned}$$

$$\begin{aligned} \text{Method 2 : } \Phi_{\text{Br}} = & \left(2k[\text{BrO}]^2 + J_{\text{BrO}}[\text{BrO}] + k[\text{BrO}][\text{ClO}] \right. \\ & + k[\text{BrO}][\text{IO}] + k[\text{BrO}][\text{CH}_3\text{OO}] \\ & + k[\text{BrO}][\text{OH}] + k[\text{BrO}][\text{O}(\text{}^3\text{P})] \\ & \left. + k[\text{BrO}][\text{CH}_3\text{COOO}] + k[\text{BrO}][\text{NO}] \right) \\ & \left(2J_{\text{Br}_2}[\text{Br}_2] + J_{\text{BrCl}}[\text{BrCl}] + J_{\text{HOBr}}[\text{HOBr}] \right. \\ & + J_{\text{BrONO}_2}[\text{BrONO}_2] + J_{\text{IBr}}[\text{IBr}] + J_{\text{BrNO}_2}[\text{BrNO}_2] \\ & + J_{\text{CHBr}_3}[\text{CHBr}_3] + k[\text{HBr}][\text{OH}] + k[\text{CH}_3\text{Br}][\text{OH}] \\ & \left. + k[\text{CHBr}_3][\text{OH}] \right) \quad (6) \end{aligned}$$

Termination reactions for bromine include those reactions that are sinks for either Br or BrO, since Br and BrO rapidly interconvert. Here, photolysis of BrO and the BrO + NO reaction is included in the numerator because they are efficient at reforming Br and propagating the chain; however, these reactions do not result in a net loss of ozone. Photolysis of BrO produces atomic oxygen that reacts with O₂ to form O₃, and NO₂ can photolyze to similarly reform O₃. Therefore, it should be noted that if we omit these reactions and consider only those that result in a net O₃ loss, it would be expected that the chain length would be shorter. Indeed, model simulations were performed without these two terms and the determined chain lengths were on average 80 % lower than those presented here. A BrO reaction with CH₃OO is included in both the numerator and denominator in Eq. (5) because this reaction has two channels, one that propagates the Br chain and one that terminates it.

In Fig. 3, we present the hourly averaged results of these calculations for the base model, which show that the two methods for calculating bromine chain length are in reasonably good agreement, although there are small differences between the two methods throughout the time series. This agreement is a test of our basic understanding of the radical chemistry. The inset graph in Fig. 3 shows a linear regression of the two methods for the chain length calculation. The

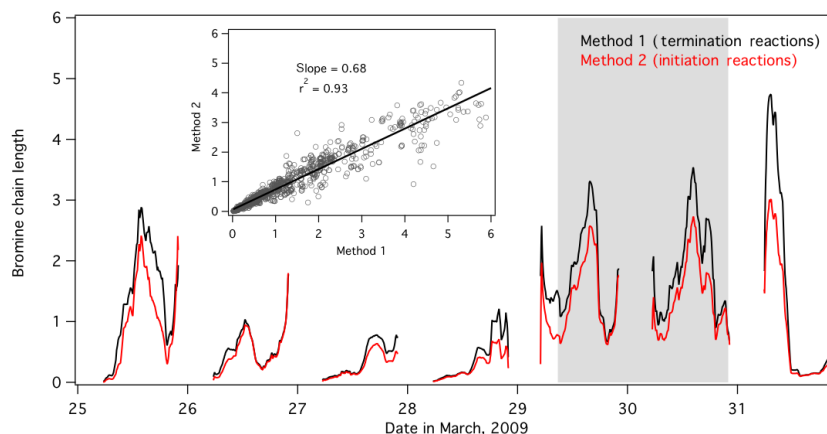


Figure 3. Time series of model-calculated bromine chain length for the daytime hours (07:00 to 21:00 AKST). Method 1 is plotted as the black trace and Method 2 is plotted as the red trace. Model output is smoothed by hourly averaging. The grey-shaded box represents a period of missing Br_2 observations. The inset graph shows a linear regression of Method 1 and Method 2 calculations. Time is expressed in Alaska standard time.

coefficient of determination (r^2) of 0.93 confirms the good temporal agreement between the two methods. However, the slope of 0.68 indicates that Method 1 is generally higher than Method 2 throughout (with some periods of exception). This offset reveals that either Method 1 is slightly overestimating the chain length or that Method 2 is underestimating it. The numerator is identical in Eqs. (5) and (6); therefore, the denominator must be driving this discrepancy, with either the denominator term in Method 1 too low or the denominator term in Method 2 too high (or some combination thereof). If it is the case that the Method 1 denominator is too low, then it must be concluded that there are important BrO_x terminations that are missing from the calculation. If, however, the denominator of Method 2 is too high, this would imply that our measurements of these BrO_x precursors are too high, which, as discussed above, is a known possibility at least for the Br_2 measurements. The photolysis of Br_2 is the dominant initiation pathway (see Sect. 3.3); therefore, the Method 2 chain length calculation would be the most sensitive to Br_2 measurement inaccuracies.

In Eq. (6), we included photolysis of the most prevalent organobromine compound bromoform for completeness, though it has been recognized for many years that the rate of Br atom production from this pathway is small (e.g., $\sim 100 \text{ molecules cm}^{-3} \text{ s}^{-1}$ for bromoform at midday) compared to Br atom production from Br_2 photolysis ($\sim 1.3 \times 10^7 \text{ molecules cm}^{-3} \text{ s}^{-1}$ at midday assuming 5 pptv of Br_2). Photolysis of bromine nitrate (BrONO_2) and nitryl bromide (BrNO_2) are also included; however, the prevalence and production of these compounds in the Arctic is highly uncertain, and no observations of these species in the Arctic have been published to date with which to compare to our modeled mixing ratios. Inclusion of these terms at the modeled BrONO_2 and BrNO_2 mixing ratios has a small effect on

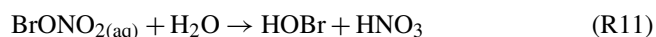
the calculated chain length that cannot account for the discrepancy between the two methods.

The median bromine chain length in the base simulation, averaging the results from Method 1 and Method 2, is ~ 1.2 across daylight hours (07:00 to 21:00 AKST) and ~ 2 for afternoon hours, defined for this purpose as approximately 12:00 to 18:00 AKST, when $[\text{O}_3] \geq 5 \text{ ppbv}$. In comparison, the bromine chain length is ~ 0.4 when $[\text{O}_3] < 5 \text{ ppbv}$ (Fig. 3). In other words, the chain cannot be maintained when $[\text{O}_3] < 5 \text{ ppbv}$. Under these conditions, Br atoms readily terminate, e.g., via reaction with CH_3CHO (see below). On 29 March there is an early morning enhancement in the chain length. This morning spike appears to correlate with a similar sharp increase in ozone. Br_2 accumulates during the nighttime hours, resulting in the highest Br_2 concentrations in the early morning hours (Fig. 1b). When the sun rises, Br_2 photolyzes rapidly, releasing a pulse of reactive bromine that converts to BrO in the presence of ozone. This, in concert with the coincident increase in ozone, can explain the enhanced chain length during the early morning hours.

Overall, midday bromine chain lengths remain near or below 2 during background O_3 days. This implies that, for these days, ozone depletion is strongly dependent upon initiation processes, and most BrO radicals produced terminate the chain via Reactions (R5) and (R10) (see below) in less than two cycles. Reaction (R12) (see below) will also efficiently terminate the chain; however, the relative importance of Reactions (R10) and (R12) depend upon the relative abundances of BrO and Br. For background O_3 days, such as 29 and 30 March, $[\text{BrO}] > [\text{Br}]$; thus, Reaction (R10) $>$ Reaction (R12). The low chain lengths calculated here are surprising, given that it has been generally accepted that Br is recycled efficiently in the gas phase. That it appears this is not the case supports the conclusions of Michalowski et al. (2000), Piot and von Glasow (2008), and

Toyota et al. (2014) that heterogeneous recycling through the “bromine explosion”, which emits Br₂ and BrCl from surface reactions, is of critical importance to sustain ODEs from occurring at the surface.

A question to address regarding the relatively small chain length calculated for Br is to what extent the chain length is dependent on NO₂. As discussed in Thompson et al. (2015) and further investigated in Custard et al. (2015), NO₂ at Barrow can be greater and more variable than at very remote sites due to its proximity to anthropogenic emissions sources. We find that the chain length calculation is relatively insensitive to NO₂ concentrations and so it is robust for the range of conditions encountered at Barrow. This is shown in detail in Custard et al. (2015). As discussed by Custard et al. (2015), while NO₂ can inhibit the bromine chain through Reactions (R10) and (R12) (i.e., decreasing the chain length), enhanced NO₂ will also reduce available HO₂, thereby decreasing the HO₂ available to terminate the chain (i.e., increasing the chain length). While the Method 2 calculation does not contain NO₂ in the denominator, the absolute [BrO] is NO_x dependent because of Reaction (R10) (Custard et al., 2015), and it is through this effect that high NO_x mixing ratios act to decrease the rate of O₃ depletion. In the natural environment, Br₂ production can potentially also be NO_x dependent, e.g., via Reaction (R11), followed by Reaction (R7). While our model does not *simulate* the condensed-phase processes, it is implicitly sensitive to them, since the model is constrained to the product of those processes, Br₂.



On the other hand, for the period of 26 through 30 March, NO_x was relatively low, and the relatively good agreement between the two calculation methods further supports our conclusion.

To investigate how chemical interactions with chlorine and iodine affect the bromine chain length, a series of simulations was performed by varying the combinations of halogens present in the model. The bromine chain length was determined for scenarios with only Br, Br and Cl (base model), Br and iodine, and base with iodine. Simulations without chlorine were performed simply by removing Cl₂, while simulations with iodine were performed by incorporating the I₂ flux as described in Sect. 2.2. No other adjustments were made to the model for these sensitivity runs.

Table 2 shows the results for both chain length calculation methods (i.e., Eqs. 5 and 6) for the different halogen combinations for the 3 days when ozone was present near background values: 25, 29, and 30 March. For the base scenario (“Br and Cl”), the average of the median daily values for the bromine chain length is 1.43 and 1.05 for Method 1 and Method 2, respectively. In comparison with the “Br Only” run, Cl chemistry does not induce a net increase in the Br

chain length, but rather causes a slight decrease. Cl chemistry can increase Br radical propagation through the addition of the BrO + ClO cross-reaction and enhancement of the BrO + CH₃OO radical propagation terms. However, Cl chemistry can also increase the concentration of reactive bromine sinks, such as aldehydes (e.g., propanal and butanal, which were free to evolve in our model; HCHO and CH₃CHO are fixed to observations) and HO₂ (see Thompson et al., 2015). Iodine has the effect of increasing the Br chain length. When low levels of iodine are added to the “Br-only” simulation, the chain increases from 1.52 to 1.59 in the Method 1 calculation, primarily due to the very fast cross-reaction between IO and BrO. The addition of Cl to the “Br and I” simulation imparts a slight decrease to the Br chain length. This may be explained by the competition between BrO and ClO for reaction with NO and/or IO, as well as the additional Br sinks in the presence of Cl chemistry. Regardless, overall there is more Br available for reaction with O₃ when Cl is present due to the interhalogen reactions, thereby increasing the rate of ozone depletion (see Thompson et al., 2015, for further discussion on ozone depletion rates).

There are several conclusions that can be drawn from Fig. 3 and Table 2: (1) there is a distinct difference in bromine chain length between O₃-depleted and non-depleted days with a significantly larger chain length when ozone is present, and (2) for all simulations, the average bromine chain is much shorter than often expected (given that gas-phase recycling has, to date, been assumed to be highly efficient). The chain length is the greatest when ozone is present because many of the species that propagate the Br chain (e.g., BrO, ClO, IO, and to a lesser extent OH and CH₃OO) require O₃ for production. Although the relationship between bromine chain length and BrO is not straightforward due to the multitude of interactions between BrO and other species that either propagate or terminate the chain, the chain length does exhibit a rough dependence on [BrO], as shown in Fig. 4, which can be loosely described with a linear fit. If it were the case that the gas-phase Br chain length was relatively long (such that the numerator far outweighs the denominator), and dominated by the BrO self-reaction, the numerator in Eqs. (5) and (6) would reduce to $2k[\text{BrO}]^2$, and the regression in Fig. 4 would display a quadratic fit; however, that is not observed here.

For purposes of comparison, the chain lengths for Cl and I were also calculated in a manner analogous to that of Eq. (5). These results are shown as hourly averages in Fig. 5 for the base with iodine scenario. It is apparent from this figure that reactive chlorine exhibits an exceptionally short chain length, whereas reactive iodine has a relatively long chain length. The average Cl chain length across the 3 days of background ozone (25, 29, and 30 March) is 0.15, or 0.23 considering only afternoon hours (12:00–18:00 AKST). This result indicates that nearly all Cl atoms that are produced terminate, likely through the very efficient reaction with a multitude of VOCs, as shown in Thompson et al. (2015). This behav-

Table 2. Median afternoon bromine chain lengths for 25, 29, and 30 March 2009 (days with O₃ present) determined for four different modeling scenarios with different combinations of halogens present. Method 1 refers to Eq. (3) (using terminations reactions) and Method 2 refers to Eq. (4) (using initiation reactions).

	25 March		29 March		30 March		Average (1 σ SD)	
	Method 1	Method 2	Method 1	Method 2	Method 1	Method 2	Method 1	Method 2
Br only	1.25	0.85	1.51	1.10	1.79	1.40	1.52 (± 0.27)	1.11 (± 0.28)
Br and Cl (base)	1.29	0.84	1.43	1.03	1.58	1.29	1.43 (± 0.14)	1.05 (± 0.22)
Br and Low I	1.37	0.86	1.60	1.12	1.82	1.41	1.59 (± 0.22)	1.13 (± 0.28)
Br, Cl, and I	1.37	0.87	1.51	1.04	1.65	1.31	1.51 (± 0.14)	1.07 (± 0.23)

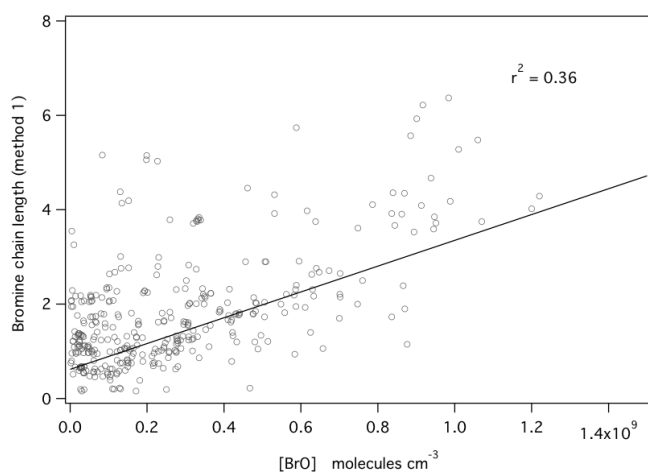


Figure 4. Regression of daytime (07:00–21:00 AKST) bromine chain length calculated by Method 1 (Eq. 5) and simulated BrO concentration.

ior also helps explain why Cl has only a small effect on the bromine chain length. In contrast, I and IO have few known sinks, which results in a reactive iodine chain length of 5.7 on average over 25, 29, and 30 March, and 7.3 over only midday hours, with maxima over 12. The high efficiency of the gas-phase regeneration of I in part explains why iodine is more efficient on a per atom basis at depleting ozone than either Br or Cl (Thompson et al., 2015).

3.3 Reactive bromine initiation, propagation, and termination pathways

The individual reactions that initiate, propagate, and terminate the reactive bromine chain were examined to determine the most important reaction pathways contributing to the chain reactions. The rates of Br atom production from the most important initiation pathways are shown as hourly averages in Fig. 6, with the y axes expressed as the cumulative rate of reaction, including all five precursors. These are reactions that produce Br atoms from stable reservoir species, which is an important distinction from the propagation reactions that produce Br atoms through radical reactions. Br₂

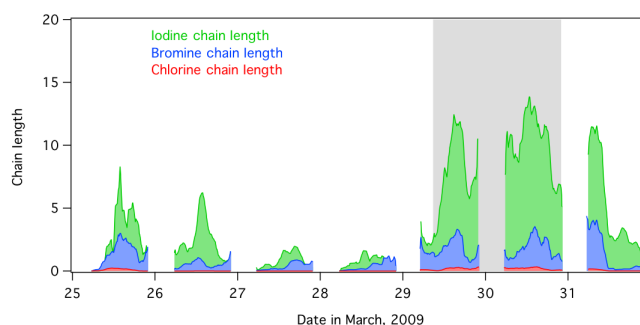


Figure 5. Calculated chain lengths for iodine (green), bromine (blue), and chlorine (red) across the 7 days of the simulated period modeled using the base + iodine scenario. Model output is smoothed by hourly averaging. The grey-shaded box represents a period of missing Br₂ observations. Time is expressed in Alaska standard time.

photolysis is calculated as $2 \times J_{\text{Br}_2} [\text{Br}_2]$. Here, we do not separate Br₂ produced in the gas-phase versus that directly emitted from a surface (this will be discussed further in Sect. 3.5). The contribution of Br₂ photolysis in producing Br atoms vastly dominates the cumulative production rate (Fig. 6a). Therefore, in Fig. 6b we show the initiation terms without Br₂ photolysis so that these other production pathways can be visualized.

Effectively, Br₂ photolysis alone controls the production of bromine atoms, while combined the remaining initiation pathways add only a minor contribution. Among the minor pathways, HOBr photolysis is the most significant during non-ODE days, with the exception of the high NO_x period of 25 March, where BrNO₂ has the largest impact. In a highly polluted environment, halogen cycling through NO_x reservoirs would become significantly more important, as has been observed with ClNO₂ in mid-latitude regions (Thornton et al., 2010; Mielke et al., 2011; Young et al., 2012). The small contribution of HOBr photolysis to bromine atom production is an important point, because the gas-phase BrO + HOBr → BrO + HO₂ ozone depletion cycle (that proceeds via HOBr photolysis rather than surface deposition) has been previously considered to be significant (see, e.g., Hausmann and Platt, 1994), though Zeng et al. (2006) noted

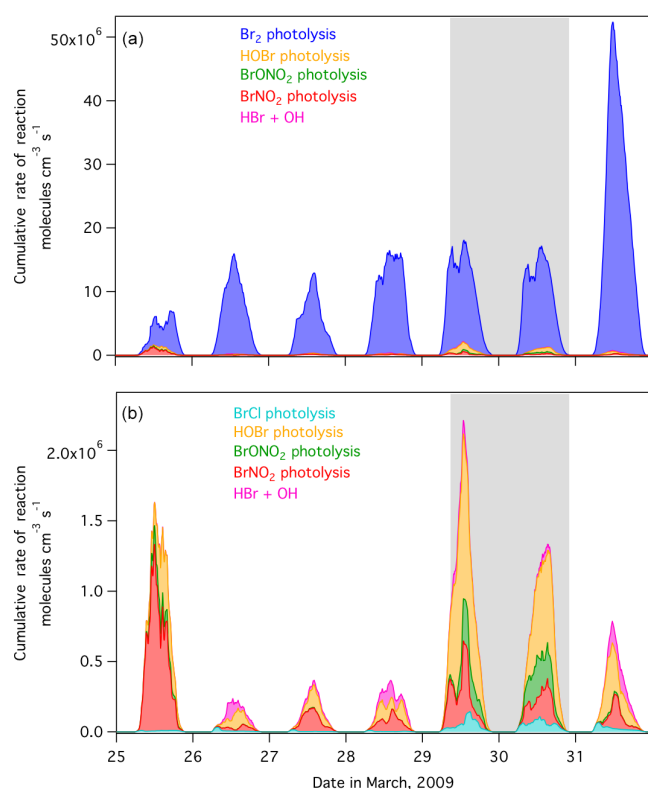


Figure 6. Time-varying rates of the most important bromine initiation reactions in the base model. Panel (a) includes photolysis of Br_2 , which dominates the bromine initiation. Br_2 photolysis is calculated as $2 \times J_{\text{Br}_2}[\text{Br}_2]$. In panel (b), Br_2 photolysis has been removed so that the minor terms can be visualized. Panel (b) also includes BrCl , which contributes only a negligible amount to bromine initiation. Model output is smoothed by hourly averaging. The y axis is expressed as a cumulative rate of reaction. The grey-shaded box represents a period of missing Br_2 observations. Time is expressed in Alaska standard time.

that HOBr photolysis has only a small effect on BrO_x cycling. Using the version of our model that is unconstrained by HOBr , but incorporates a larger surface deposition in order to reproduce observations (Fig. 2c), we were able to determine that photolysis accounts for 19 % of the HOBr sink integrated over the 7-day simulation period. Surface deposition accounts for 80 %, and other known gas-phase reactions ($\text{HOBr} + \text{Br}$, $\text{HOBr} + \text{Cl}$, $\text{HOBr} + \text{OH}$, $\text{HOBr} + \text{O}$) are only minor sink terms at a combined 1 %.

The cumulative rates of reaction of the most important propagation pathways, with and without iodine, are shown in Fig. 7a and b. The rate of the $\text{BrO} + \text{BrO}$ reaction is calculated as $2k[\text{BrO}]^2$, since this reaction results in the production of two Br atoms. The reaction pathways that dominate the bromine propagation, i.e., BrO photolysis and reaction with NO , are those that do not result in a net ozone loss. This has been previously recognized and applied to Br steady-state calculations in several works (e.g., Platt and Janssen,

1995; Zeng et al., 2006; Holmes et al., 2010), and demonstrates that much of the time BrO regenerates Br without a net loss of ozone for the simulated conditions in Barrow. Indeed, in our previous paper, we calculated that ~ 70 % of gas-phase BrO reforms ozone via photolysis or reaction with NO over this period (Thompson et al., 2015). The inset pie charts, which show the average fractional importance of the various propagation reactions for 29 and 30 March, reveal that these two pathways account for 88–91 % of the total. Interestingly, the BrO self-reaction is small in comparison, with an average contribution of 5–6 %, and a maximum of 46 %. However, if we consider only those reactions that *do* lead to a net ozone loss, then the BrO self-reaction accounts for an average of 71 % and a maximum of 98 % of the propagation. The rate of the $\text{BrO} + \text{ClO}$ reaction rate is much smaller than that for $\text{BrO} + \text{BrO}$, though not insignificant. While on average this reaction pathway accounts for only 2 %, it does reach 16 % when Cl_2 is high on 29 March. In considering only those reactions that result in a net ozone loss, the $\text{BrO} + \text{ClO}$ pathway accounts for 21 % on average, and up to a maximum of 57 %. In panel b, the base with iodine scenario is shown. At these levels, the $\text{BrO} + \text{IO}$ reaction accounts for 4 % of the propagation, which is at times comparable to $\text{BrO} + \text{BrO}$ and greater than $\text{BrO} + \text{ClO}$, even at the low IO mixing ratios in this simulation (~ 1 pptv).

The short gas-phase chain length calculated for bromine propagation indicates that there are large reactive bromine (BrO_x) sinks terminating the chain reaction. Figure 8 presents the rates of the most important BrO_x termination reactions, with the y axis expressed as the cumulative rate of reaction. Here it can be seen that reaction of BrO with NO_2 is the dominant sink for BrO_x on non-ODE days for the conditions encountered at Barrow, while Br reaction with CH_3CHO is most important when O_3 is depleted. That HO_2 is a significant sink, and would be more so in less anthropogenically impacted polar regions, points toward the importance of heterogeneous recycling through the bromine explosion mechanism. During ozone depletion, such as the major event from the days 26 to 28 March ($[\text{O}_3] < 5$ ppbv) when BrO is mostly absent, CH_3CHO becomes the primary sink term for Br, and HCHO is relatively more important. The strength of the CH_3CHO sink is much greater than is HCHO , as noted previously by Shepson et al. (1996) and Bottenheim et al. (1990). Of note are the relatively similar magnitudes for the total rate of reaction of the initiation, propagation, and termination reactions shown in Figs. 6, 7, and 8, respectively, which of course must be the case for a chain length near 1. This accounts for the short bromine chain length determined here and also indicates that to sustain elevated bromine radical concentrations necessary to deplete O_3 requires a relatively large Br_2 source, likely in the form of a significant flux of Br_2 from the snow surface, or from in situ production from aerosols.

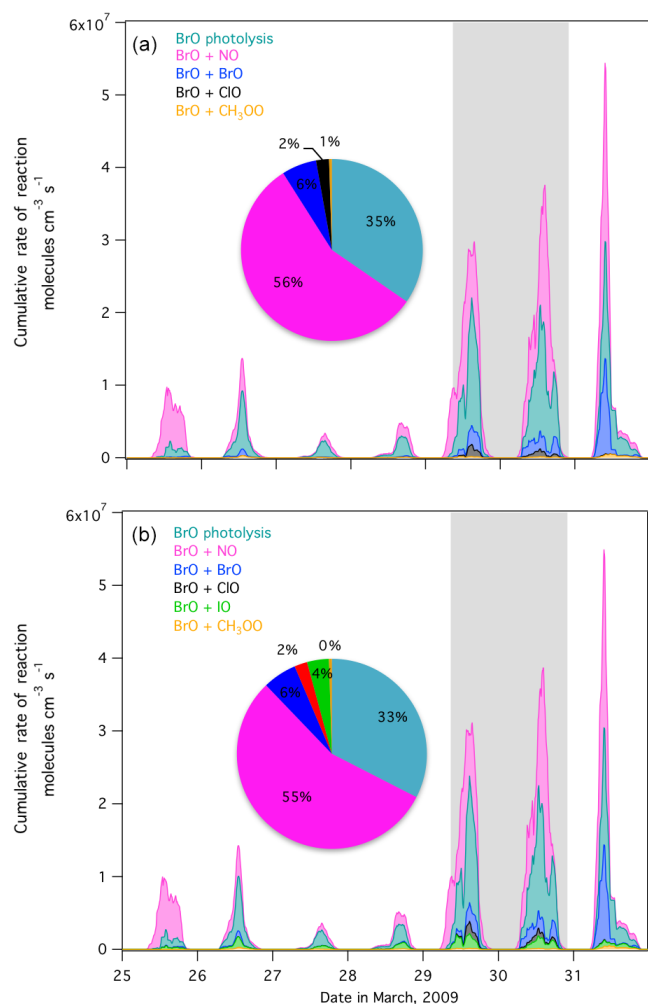


Figure 7. Time-varying rates of the most important bromine propagation reactions in the base model with Br and Cl present (a) and with iodine included (b). The BrO + BrO reaction is calculated as $2k[\text{BrO}]^2$ as this reaction regenerates two Br atoms. Model output is smoothed by hourly averaging. The y axis is expressed as a cumulative rate of reaction. The grey-shaded box represents a period of missing Br₂ observations. Time is expressed in Alaska standard time. The inset pie charts show the average fractional importance of each reaction pathway for only the days of 29 and 30 March (i.e., background O₃ days).

3.4 Ozone loss rate

Since the chain length calculations suggest a larger than expected contribution of heterogeneous bromine recycling to Br atom production, to examine this further, we calculated the rate of net ozone loss by Br and Cl in the base model using Eq. (7) and compared this rate to that using the estimation method presented in previous works as shown in Eq. (2) (Platt and Janssen, 1995; Le Bras and Platt, 1995). Additionally, the total simulated chemical ozone loss in the base model was calculated from Eq. (8), which includes O₃

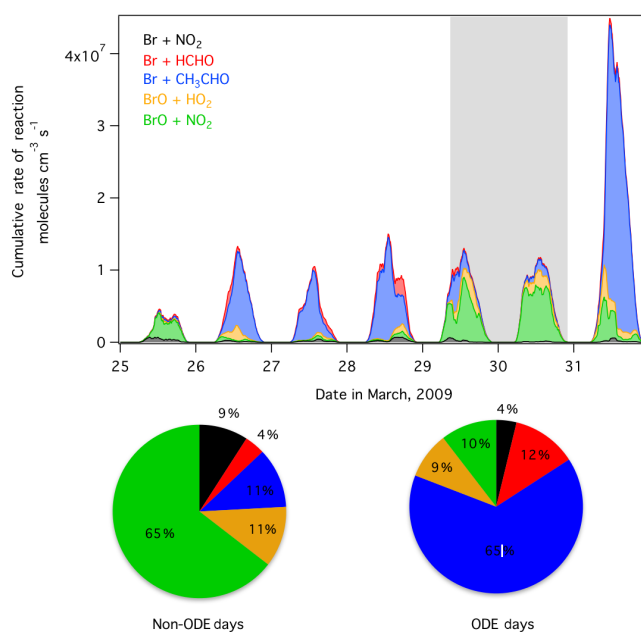


Figure 8. Time-varying rates of the most important reactive bromine (BrO_x) termination reactions in the base model. Model output is smoothed by hourly averaging. The y axis is expressed as a cumulative rate of reaction. The grey-shaded box represents a period of missing Br₂ observations. Time is expressed in Alaska standard time. The pie charts show the average fractional importance of each reactive bromine sink for non-ODE (background O₃) days and ODE days.

destruction by OH, HO₂, and photolysis (determined here as $k[\text{O}(^1\text{D})][\text{H}_2\text{O}]$).

$$\text{O}_3 \text{ Loss by Br and Cl} = \left(k[\text{Br}][\text{O}_3] - J[\text{BrO}] - k[\text{BrO}][\text{NO}] \right) + \left(k[\text{Cl}][\text{O}_3] - J[\text{ClO}] - k[\text{ClO}][\text{NO}] \right) \quad (7)$$

$$\text{Total Chemical O}_3 \text{ loss Rate} = k[\text{Br}][\text{O}_3] + k[\text{Cl}][\text{O}_3] + k[\text{O}(^1\text{D})][\text{H}_2\text{O}] + k[\text{OH}][\text{O}_3] + k[\text{HO}_2][\text{O}_3] - k[\text{BrO}][\text{NO}] - J[\text{BrO}] - k[\text{ClO}][\text{NO}] - J[\text{ClO}] \quad (8)$$

The method in Eq. (2) assumes that the rate of ozone loss is equivalent to the rate at which Br is regenerated through BrO reaction with itself and ClO (thus assuming efficient gas-phase propagation and a long chain length), whereas Eq. (7) accounts for all net ozone destruction by Br and Cl, by correcting for those reactions that release a triplet oxygen atom and reform O₃. In other words, this method accounts for the fact that some BrO radicals react to terminate the chain (and at steady state, an equivalent BrO_x production rate is necessary). Figure 9a compares these two estimations for O₃ loss rate in green (Eq. 2) and pink (Eq. 7). This comparison clearly shows that there is a large difference between the methods, with the estimation from Eq. (2) significantly smaller overall. Additionally, the total chemical O₃ loss (calculated by Eq. 8) is shown in the dashed black trace. The O₃

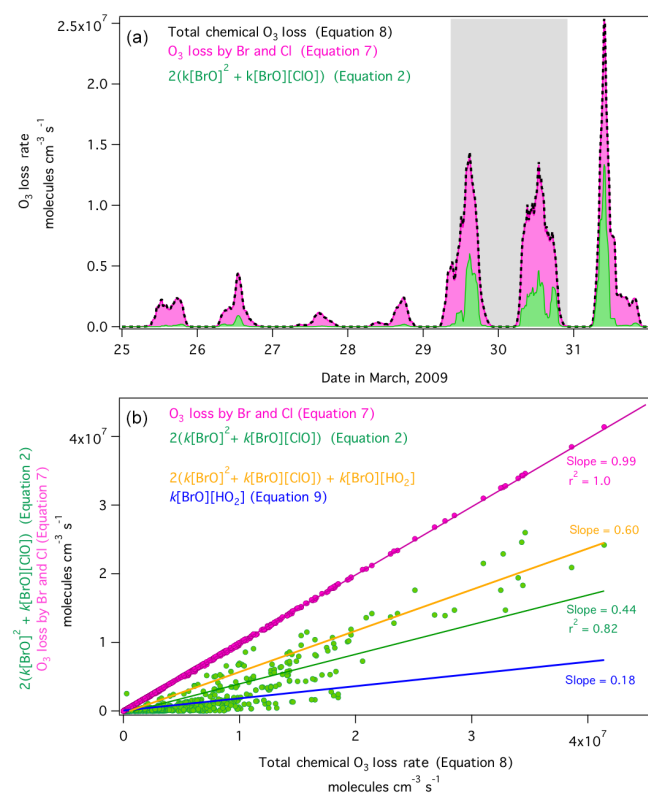


Figure 9. (a) Comparison of the time-varying O₃ loss rate calculated using the estimation of $2(k[\text{BrO}]^2 + k[\text{BrO}][\text{ClO}])$ (Eq. 2, green), the simulated O₃ loss rate by Br and Cl (Eq. 7, pink), and the total simulated chemical O₃ loss rate (Eq. 8, dashed black trace). Model output is smoothed by hourly averaging. The grey-shaded box represents a period of missing Br₂ observations. Time is expressed in Alaska standard time. (b) Shown is a regression of the $2(k[\text{BrO}]^2 + k[\text{BrO}][\text{ClO}])$ estimation method (Eq. 2) versus the total simulated chemical O₃ loss rate in the base model (Eq. 8) in the green data, and a regression of O₃ loss rate by Br and Cl only (Eq. 7) versus the total simulated chemical O₃ loss rate in the pink data. The blue trace represents the O₃ loss rate estimated by only considering $k[\text{BrO}][\text{HO}_2]$ (Eq. 9). The orange trace estimates O₃ loss rate combining the three major gas-phase ozone depletion cycles. The slopes represent the fraction of the chemical O₃ loss rate that can be accounted for by each method. For the conditions simulated, the commonly used estimation method of $2(k[\text{BrO}]^2 + k[\text{BrO}][\text{ClO}])$ only accounts for 44 % of the chemical O₃ loss rate.

loss rate estimation presented in Eq. (7) accounts for nearly all of the chemical O₃ loss (i.e., most chemical O₃ loss is a result of halogen chemistry), such that the dashed black line lies nearly perfectly on top of the pink-shaded regions.

In Fig. 9b, we show a regression of the two estimation methods (Eq. 2 in green and Eq. 7 in pink) versus the total chemical O₃ loss rate (Eq. 8). Here it can be seen from the pink data that halogen chemistry accounts for 99 % of the total chemical O₃ loss under the conditions simulated here. Importantly, the O₃ loss rate estimation presented in Eq. (2) accounts for only 44 % of the total chemical O₃ loss rate.

In the work by Hausmann and Platt (1994), the authors also considered the $\text{BrO} + \text{HO} \rightarrow \text{Br} + \text{HO}_2$ gas-phase ozone depletion cycle as a proxy for estimating the O₃ loss rate, using the equation shown below (Eq. 17 of Hausmann and Platt, 1994).

$$\frac{d[\text{O}_3]}{dt} = (k_5 \cdot [\text{BrO}] \cdot [\text{HO}_2]) \quad (9)$$

The authors only considered the gas-phase cycle of HOBr here with the photolysis of HOBr regenerating Br. At the time of this publication, the heterogeneous cycling of HOBr had only recently been proposed and had not been fully validated. Hausmann and Platt (1994) showed that Eq. (9) resulted in a significantly lower estimation for O₃ depletion than did Eq. (1), which considered only the BrO–BrO cycle. In Fig. 9b, we show also the O₃ loss rate estimated using Eq. (9) in blue. Our results corroborate that of Hausmann and Platt (1994), and demonstrate that Eq. (9) can account for only 18 % of the O₃ loss. To examine this one step further, we present an additional regression in Fig. 8b (orange trace) that combines Eqs. (2) and (9), thereby considering the three predominant gas-phase O₃ depletion cycles of BrO–BrO, BrO–ClO, and BrO–HO₂. This still can only account for 60 % of the O₃ loss.

Our analysis quantitatively expresses the conclusion that the gas-phase recycling of bromine is not as efficient as previously considered and that it is often the case, for Barrow, that BrO_x terminations must often, through Reactions (R5) or (R10), be followed by heterogeneous production of Br₂ through condensed-phase reactions of HOBr and/or BrONO₂. In other words, the reproduction of Br₂ via reactive deposition/uptake of HOBr and/or BrONO₂ onto surfaces, followed by their gas-phase production via $\text{BrO} + \text{HO}_2$ and $\text{BrO} + \text{NO}_2$, respectively, plays a significant role in the catalytic ozone loss involving Br atoms in the Arctic boundary layer. An important conclusion from this analysis is that the chemical O₃ loss rate is largely underestimated when calculated from only BrO observations using the previously accepted $2(k[\text{BrO}]^2 + k[\text{BrO}][\text{ClO}])$ method, and one should be cautious about drawing conclusions about O₃ depletion rates and timescales based solely on BrO observations. This may have significant impacts on the process of examining ODEs and addressing the extent to which they represent local scale chemistry versus transport effects. While this situation is significantly impacted by local NO_x sources at Barrow, NO_x is expected to increase with development around the Arctic.

3.5 Bromine atom production

If it is the case that heterogeneous recycling is of such importance, it may be that Reaction (R5) ($\text{BrO} + \text{HO}_2$) competes favorably with Reaction (R3) ($\text{BrO} + \text{BrO}$). Panel A of Fig. 10 shows the rates of Reactions (R5) and (R3). This plot demonstrates that for our modeling results, the rate of reac-

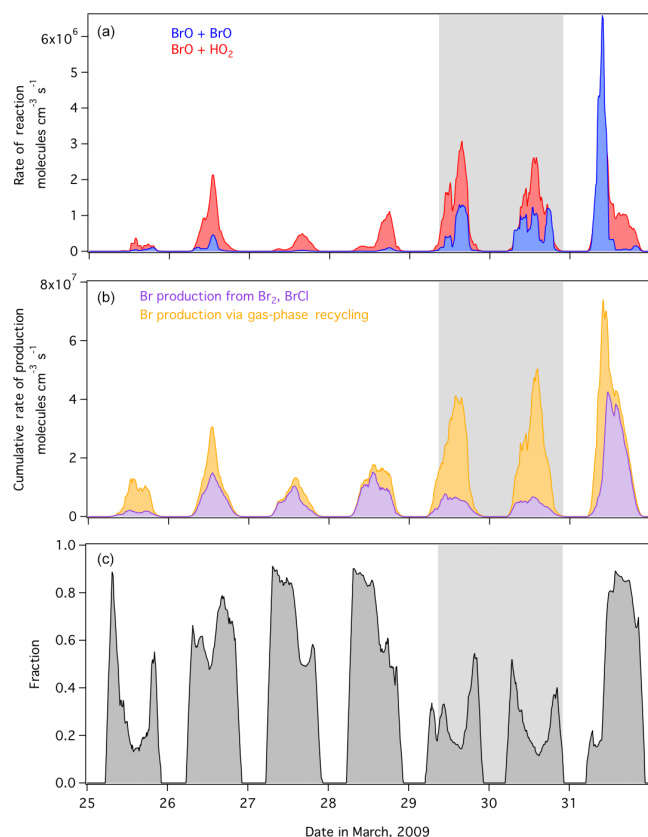


Figure 10. (a) Comparison of the rate of reaction of BrO + BrO (blue) and BrO + HO₂ (red). (b) The cumulative rate of Br atom production separated into the Br production rate from the photolysis of Br₂ and BrCl surface emissions calculated from Eq. (10) (purple) and the Br atom production rate due to gas-phase radical recycling calculated from Eq. (11) (orange). (c) The fraction of total Br atom production due to production from Br₂ and BrCl surface emissions. In all panels, model output is smoothed by hourly averaging. The grey-shaded box represents a period of missing Br₂ observations. Time is expressed in Alaska standard time.

tion of BrO with HO₂ is often of a comparable or greater magnitude than the BrO self-reaction, and remains significant throughout the simulated period. Previous modeling work by Sander et al. (1997) also compared the rates of these two critical reactions (Fig. 2 of that work). In contrast to our results, their model predicted that the rate of the BrO + BrO reaction was up to a factor of 8 greater than that of BrO + HO₂. The reason for this difference may perhaps be the much lower mixing ratios of HO₂ in the model by Sander et al. (1997). Their model predicted HO₂ daily maxima of 0.2 to 0.6 pptv for most days, increasing to 1.8 pptv on the final 3 days of their simulation. In contrast, HO₂ observations at Barrow were frequently greater than 5 and up to 10 pptv. As demonstrated in Thompson et al. (2015), HCHO was a dominant factor in controlling the HO₂ mixing ratios in Barrow. The low levels of HO₂ in Sander et al. (1997) likely also contribute to their low predicted HOBr mixing ra-

tios, which do not exceed 1 pptv in their model. This also is much lower than observations at Barrow, where HOBr reaching 10 to 20 pptv was measured during our simulated period. Because the BrO + HO₂ reaction is of primary importance for the bromine explosion mechanism, our result supports the hypothesis that heterogeneous recycling may be equally, or even more, important than gas-phase recycling of reactive bromine.

Given that the chain length is small, it must be that initiation is an important source of Br atoms in order to sustain BrO and lead to O₃ depletion. To further examine the question of surface emissions/release versus gas-phase recycling, we determined the rate of production of Br atoms via photolysis of Br₂ and BrCl (Eq. 10) compared to the rate of production of Br atoms through gas-phase recycling calculated by Eq. (11). Because our model is constrained by Br₂ observations and we do not produce Br₂ from surfaces via heterogeneous reactions, the photolysis of Br₂ includes Br₂ that is both emitted from surfaces and that is formed via gas-phase reactions. To correct for the Br₂ that is formed in the gas-phase reactions so that Eq. (10) represents our best approximation for surface-emitted Br₂, we created a proxy in the model, Br₂^{*}, which represents the Br₂ produced from gas-phase reactions. These reactions include Br + BrNO₂, Br + BrONO₂, and the BrO + BrO branch that produces Br₂. Equation (10) is thus corrected for the gas-phase generated Br₂ by subtracting the photolysis of Br₂^{*}. A comparison of Br₂ and Br₂^{*} reveals that these three gas-phase production pathways account for an average of 35 % of observed Br₂, suggesting that the snowpack and/or aerosols emit the remaining 65 %. Again, we cannot distinguish between snow or aerosol production using this method.

Br Production from Surface-derived Br₂, BrCl

$$= 2 \times J_{\text{Br}_2}[\text{Br}_2] + J_{\text{BrCl}}[\text{BrCl}] - 2 \times J_{\text{Br}_2}[\text{Br}_2^*] \quad (10)$$

Br Production via Gas-phase Recycling

$$\begin{aligned} &= 2k[\text{BrO}][\text{BrO}] + k[\text{BrO}][\text{ClO}] \\ &+ k[\text{BrO}][\text{NO}] + k[\text{BrO}][\text{OH}] + k[\text{BrO}][\text{O}(\text{P})] \\ &+ k[\text{BrO}][\text{CH}_3\text{OO}] + k[\text{BrO}][\text{CH}_3\text{COOO}] \\ &+ J_{\text{HOBr}}[\text{HOBr}] + J_{\text{BrO}}[\text{BrO}] + J_{\text{BrONO}_2}[\text{BrONO}_2] \\ &+ J_{\text{BrNO}_2}[\text{BrNO}_2] \end{aligned} \quad (11)$$

Figure 10b compares the results of Eqs. (10) and (11), showing the total rate of Br atom production separated into Br production from the derived “surface-emitted” Br₂ and BrCl (purple) and from gas-phase Br recycling (orange); panel c plots the fraction of total Br atom production that is due to production from Br₂ and BrCl surface emissions/release. The majority of the time during this 7-day period Br atom production from Br₂ and BrCl emissions/release (Eq. 10) accounts for 30 % or greater of the total, and at times reaches up to 90 %. This explains both how ozone depletion can be rapid despite the short calculated bromine radical chain length, as well as the difference found between the two methods of esti-

ating O₃ loss rate in Fig. 9. Therefore, it is concluded from this analysis that the condensed-phase recycling of bromine can be of equal or greater importance to the evolution of ODEs than gas-phase Br regeneration through radical recycling reactions.

4 Conclusions

The analysis presented here suggests that the gas-phase recycling of bromine species may be less important than commonly believed, and we conclude that heterogeneous recycling is critical for the evolution of ODEs/AMDEs, consistent with results by Michalowski et al. (2000), Piot and von Glasow (2008), and Toyota et al. (2011, 2014). Expressed in another way, the reproduction of Br₂ via reactive deposition/uptake of HOBr and/or BrONO₂ onto surfaces, followed by their gas-phase production via BrO + HO₂ and BrO + NO₂, respectively, is critical for sustaining the Br atom chemistry leading to O₃ depletion in the Arctic boundary layer.

To support this conclusion, we have used the gas-phase bromine chain length, which had not previously been applied to Arctic halogen chemistry, as an objective metric. The gas-phase bromine chain length is much shorter than expected, suggesting that much of the Br present in the gas-phase is Br from surface emissions/release. Again note that our calculation of chain length includes photolysis of BrO and BrO + NO, which do not result in net O₃ loss. Had we omitted these two reactions, which we have found are in fact dominating the radical propagation, the chain length would be, on average, 80 % shorter. Because of the small chain length calculated for Br, one must be cautious about drawing conclusions about O₃ depletion from BrO measurements alone. We recommend concurrent measurements of a broad suite of inorganic bromine species for accurate study of these ozone depletion events. The very low mixing ratios of HOBr predicted by Sander et al. (1997) and the high mixing ratios originally predicted by our model point to the need for measurements of these species to validate the accuracy of Arctic models.

We find that between 30 and 90 % of Br atoms are produced from surface emissions/release of Br₂ and BrCl, though we cannot distinguish snow sources from aerosol sources using our model. However, it is important to note that we do not know how much of the condensed-phase Br₂ production derives from Reaction (R7), or from some other condensed-phase process, e.g., oxidation of Br⁻ by OH radicals (Abbatt et al., 2010). The in situ snow chamber experiments by Pratt et al. (2013) demonstrated a strong Br₂ source from the snowpack; similar field observations proving significant Br₂ release from Arctic aerosol are currently lacking. If the snow surface is the primary source of these emissions, then a strong vertical gradient would be expected in the near-surface boundary layer, and our estimations for

the Br chain length would be only valid for the height of our measurements (~ 1 m above the snow). Strong deposition to the snow would also induce a vertical gradient in these species. If, however, aerosols are an important source of Br₂ (or other halogen precursors), then Br₂ production should occur throughout the entire height of the boundary with no significant vertical gradient, in a similar fashion as has been observed for ClNO₂, which is a known product of aerosol chemistry (Young et al., 2012). It is clear that vertically resolved measurements of these halogen precursors are imperative for our understanding of halogen production in the Arctic.

The production of Br₂ is quite complex and is dependent on many factors, including the relative concentrations of bromide and chloride (among others), the availability of atmospheric oxidants, such as ozone (e.g., Oum et al., 1998; Pratt et al., 2013), the pH of the snow surfaces or aerosol (Toyota et al., 2011, 2014), the presence of snow-phase oxidants such as H₂O₂ (Pratt et al., 2013), and the replenishment of the snowpack halides from deposited sea salts. The last of these is governed by meteorology, the proximity of open water or saline sea ice surfaces, and wind/storm events, making the accurate modeling of these processes very complex (Domine et al., 2013). Likewise, to date, it has not been possible to determine the halide concentrations or pH of the snow grain surfaces, and these values are likely highly variable and dependent on snow and aerosol aging and deposition of atmospheric constituents. Due to the apparent importance of surface chemistry for both the initiation and evolution of Arctic ozone depletion events, it is clear that more laboratory and field studies are required to decipher these complex chemical and physical processes. In particular, we strongly recommend studies relating to direct measurements of surface fluxes of molecular halogens, as a function of conditions of temperature, snowpack composition, and pH, as well as deposition velocities for the hypohalous acids (HOBr, HOCl) to the snow. Our model overestimation of HOBr, which necessitated constraint to observations, suggests a sometimes much stronger, but also variable, deposition of HOBr that is currently unknown. Further, there is currently little understanding of the mechanism for Cl₂ production in the Arctic, and no successful measurements of IO in the High Arctic. Recent observations of I₂ within the Barrow snowpack (Raso et al., 2017) suggest reactive iodine chemistry is present in this region, and this would have an impact on Br recycling and ozone depletion rate. Investigations into these areas would greatly increase our understanding of halogen chemistry and ozone depletion in the Arctic.

Data availability. Data sets from the OASIS 2009 campaign are archived individually on the NSF Arctic Data Center site (<https://arcticdata.io>) under multiple digital object identifiers all searchable using the search term "OASIS". Data sets are additionally archived on the NCAR EOL website (<https://doi.org/10.5065/D6CJ8BM3>).

Competing interests. The authors declare that they have no conflict of interest.

Acknowledgements. This work was funded by the National Science Foundation grant ARC-0732556. Partial support for CT during preparation of this manuscript was provided by the NSF Atmospheric and Geospace Sciences Postdoctoral Research Fellowship program. The authors wish to thank the organizers of the OASIS 2009 field campaign, the Barrow Arctic Science Consortium for logistics support, and all of the researchers, who contributed to the campaign. This paper is submitted in memory of our colleague and friend, Roland von Glasow.

Edited by: P. Monks

Reviewed by: two anonymous referees

References

- Abbatt, J., Oldridge, N., Symington, A., Chukalovskiy, V., McWhinney, R. D., Sjostedt, S., and Cox, R. A.: Release of Gas-Phase Halogens by Photolytic Generation of OH in Frozen Halide–Nitrate Solutions: An Active Halogen Formation Mechanism?, *J. Phys. Chem. A*, 114, 6527–6533, doi:10.1021/jp102072t, 2010.
- Abbatt, J. P. D., Thomas, J. L., Abrahamsson, K., Boxe, C., Granfors, A., Jones, A. E., King, M. D., Saiz-Lopez, A., Shepson, P. B., Sodeau, J., Toohey, D. W., Toubin, C., von Glasow, R., Wren, S. N., and Yang, X.: Halogen activation via interactions with environmental ice and snow in the polar lower troposphere and other regions, *Atmos. Chem. Phys.*, 12, 6237–6271, doi:10.5194/acp-12-6237-2012, 2012.
- Adams, J. W., Holmes, N. S., and Crowley, J. N.: Uptake and reaction of HOBr on frozen and dry NaCl/NaBr surfaces between 253 and 233 K, *Atmos. Chem. Phys.*, 2, 79–91, doi:10.5194/acp-2-79-2002, 2002.
- Apel, E., Emmons, L., Karl, T., Flocke, F., Hills, A., Madronich, S., Lee-Taylor, J., Fried, A., Weibring, P., and Walega, J.: Chemical evolution of volatile organic compounds in the outflow of the Mexico City metropolitan area, *Atmos. Chem. Phys.*, 10, 2353–2375, doi:10.5194/acp-10-2353-2010, 2010.
- Aranda, A., Le Bras, G., La Verdet, G., and Poulet, G.: The BrO⁺ CH₃O₂ reaction: Kinetics and role in the atmospheric ozone budget, *Geophys. Res. Lett.*, 24, 2745–2748, doi:10.1029/97GJ02686, 1997.
- Ariya, P., Jobson, B., Sander, R., Niki, H., Harris, G., Hopper, J., and Anlauf, K.: Measurements of C₂–C₇ hydrocarbons during the Polar Sunrise Experiment 1994: Further evidence for halogen chemistry in the troposphere, *J. Geophys. Res.*, 103, 13169–13180, 1998.
- Atkinson, R., Baulch, D. L., Cox, R. A., Crowley, J. N., Hampson, R. F., Hynes, R. G., Jenkin, M. E., Rossi, M. J., and Troe, J.: Evaluated kinetic and photochemical data for atmospheric chemistry: Volume I – gas phase reactions of O_x, HO_x, NO_x and SO_x species, *Atmos. Chem. Phys.*, 4, 1461–1738, doi:10.5194/acp-4-1461-2004, 2004.
- Atkinson, R., Baulch, D. L., Cox, R. A., Crowley, J. N., Hampson, R. F., Hynes, R. G., Jenkin, M. E., Rossi, M. J., Troe, J., and IUPAC Subcommittee: Evaluated kinetic and photochemical data for atmospheric chemistry: Volume II – gas phase reactions of organic species, *Atmos. Chem. Phys.*, 6, 3625–4055, doi:10.5194/acp-6-3625-2006, 2006.
- Atkinson, R., Baulch, D. L., Cox, R. A., Crowley, J. N., Hampson, R. F., Hynes, R. G., Jenkin, M. E., Rossi, M. J., and Troe, J.: Evaluated kinetic and photochemical data for atmospheric chemistry: Volume III – gas phase reactions of inorganic halogens, *Atmos. Chem. Phys.*, 7, 981–1191, doi:10.5194/acp-7-981-2007, 2007.
- Barrie, L., Bottenheim, J., Schnell, R., Crutzen, P., and Rasmussen, R.: Ozone destruction and photochemical reactions at polar sunrise in the lower Arctic atmosphere, *Nature*, 334, 138–141, doi:10.1038/334138a0, 1988.
- Beckwith, R. C., Wang, T. X., and Margerum, D. W.: Equilibrium and kinetics of bromine hydrolysis, *Inorg. Chem.*, 35, 995–1000, 1996.
- Bottenheim, J. W., Barrie, L. A., Atlas, E., Heidt, L. E., Niki, H., Rasmussen, R. A., and Shepson, P. B.: Depletion of lower tropospheric ozone during Arctic spring: The Polar Sunrise Experiment 1998, *J. Geophys. Res.*, 95, 18555–18568, 1990.
- Calvert, J. G. and Lindberg, S. E.: Potential influence of iodine-containing compounds on the chemistry of the troposphere in the polar spring. I. Ozone depletion, *Atmos. Environ.*, 38, 5087–5104, doi:10.1016/j.atmosenv.2004.05.049, 2004.
- Cao, L., Sihler, H., Platt, U., and Gutheil, E.: Numerical analysis of the chemical kinetic mechanisms of ozone depletion and halogen release in the polar troposphere, *Atmos. Chem. Phys.*, 14, 3771–3787, doi:10.5194/acp-14-3771-2014, 2014.
- Cavender, A. E., Biesenthal, T. A., Bottenheim, J. W., and Shepson, P. B.: Volatile organic compound ratios as probes of halogen atom chemistry in the Arctic, *Atmos. Chem. Phys.*, 8, 1737–1750, doi:10.5194/acp-8-1737-2008, 2008.
- Clyne, M. and Cruse, H.: Atomic resonance fluorescence spectrometry for the rate constants of rapid bimolecular reactions, Part 2. Reactions Cl⁺ BrCl, Cl⁺ Br₂, Cl⁺ ICl, Br⁺ IBr, Br⁺ ICl, *J. Chem. Soc., Faraday Trans. 2*, 68, 1377–1387, 1972.
- Custard, K. D., Thompson, C. R., Pratt, K. A., Shepson, P. B., Liao, J., Huey, L. G., Orlando, J. J., Weinheimer, A. J., Apel, E., Hall, S. R., Flocke, F., Mauldin, L., Hornbrook, R. S., Pöhler, D., General, S., Zielcke, J., Simpson, W. R., Platt, U., Fried, A., Weibring, P., Sive, B. C., Ullmann, K., Cantrell, C., Knapp, D. J., and Montzka, D. D.: The NO_x dependence of bromine chemistry in the Arctic atmospheric boundary layer, *Atmos. Chem. Phys.*, 15, 10799–10809, doi:10.5194/acp-15-10799-2015, 2015.
- Domine, F., Bock, J., Voisin, D., and Donaldson, D. J.: Can We Model Snow Photochemistry? Problems with the Current Approaches, *J. Phys. Chem., A*, 117, 4733–4749, doi:10.1021/jp3123314, 2013.
- Edwards, G. D., Cantrell, C. A., Stephens, S., Hill, B., Goyea, O., Shetter, R. E., Mauldin III, R. L., Kosciuch, E., Tanner, D. J., and Eisele, F. L.: Chemical ionization mass spectrometer instrument for the measurement of tropospheric HO₂ and RO₂, *Anal. Chem.*, 75, 5317–5327, doi:10.1021/ac034402b, 2003.
- Ehhalt, D. H.: Photooxidation of trace gases in the troposphere Plenary Lecture, *Phys. Chem. Chem. Phys.*, 1, 5401–5408, 1999.
- Fan, S.-M. and Jacob, D. J.: Surface ozone depletion in Arctic spring sustained by bromine reactions on aerosols, *Nature*, 358, 522–524, 1992.

- Foster, K. L., Plastring, R. A., Bottenheim, J. W., Shepson, P. B., Finlayson-Pitts, B. J., and Spicer, C. W.: The role of Br₂ and BrCl in surface ozone destruction at polar sunrise, *Science*, 291, 471–474, 2001.
- Fried, A., Sewell, S., Henry, B., Wert, B. P., and Gilpin, T.: Tunable diode laser absorption spectrometer for ground-based measurements of formaldehyde, *J. Geophys. Res.*, 102, 6253–6266, doi:10.1029/96JD01580, 1997.
- Gladich, I., Francisco, J. S., Buszek, R. J., Vazdar, M., Caignano, M. A., and Shepson, P. B.: *Ab Initio* Study of the Reaction of Ozone with Bromide Ion, *J. Phys. Chem. A*, 119, 4482–4488, 2015.
- Gong, S., Walmsley, J., Barrie, L., and Hopper, J.: Mechanisms for surface ozone depletion and recovery during polar sunrise, *Atmos. Environ.*, 31, 969–981, 1997.
- Guimbaud, C., Grannas, A. M., Shepson, P. B., Fuentes, J. D., Boudries, H., Bottenheim, J. W., Dominé, F., Houdier, S., Perrier, S., and Biesenthal, T. B.: Snowpack processing of acetaldehyde and acetone in the Arctic atmospheric boundary layer, *Atmos. Environ.*, 36, 2743–2752, 2002.
- Hansen, J. C., Li, Y., Li, Z., and Francisco, J. S.: On the mechanism of the BrO+ HBr reaction, *Chem. Phys. Lett.*, 314, 341–346, doi:10.1016/S0009-2614(99)01093-3, 1999.
- Hausmann, M. and Platt, U.: Spectroscopic measurement of bromine oxide and ozone in the high Arctic during Polar Sunrise Experiment 1992, *J. Geophys. Res.*, 99, 25399, doi:10.1029/94JD01314, 1994.
- Helmig, D., Ganzeveld, L., Butler, T., and Oltmans, S. J.: The role of ozone atmosphere-snow gas exchange on polar, boundary-layer tropospheric ozone – a review and sensitivity analysis, *Atmos. Chem. Phys.*, 7, 15–30, doi:10.5194/acp-7-15-2007, 2007.
- Helmig, D., Boylan, P., Johnson, B., Oltmans, S., Fairall, C., Staebler, R., Weinheimer, A., Orlando, J., Knapp, D. J., Montzka, D. D., Flocke, F., Frieß, U., Sihler, H., and Shepson, P. B.: Ozone dynamics and snow-atmosphere exchanges during ozone depletion events at Barrow, Alaska, *J. Geophys. Res.*, 117, D20303, doi:10.1029/2012JD017531, 2012.
- Hirokawa, J., Onaka, K., Kajii, Y., and Akimoto, H.: Heterogeneous processes involving sodium halide particles and ozone: molecular bromine release in the marine boundary layer in the absence of nitrogen oxides, *Geophys. Res. Lett.*, 25, 2449–2452, 1998.
- Holmes, C. D., Jacob, D. J., Corbitt, E. S., Mao, J., Yang, X., Talbot, R., and Slemr, F.: Global atmospheric model for mercury including oxidation by bromine atoms, *Atmos. Chem. Phys.*, 10, 12037–12057, doi:10.5194/acp-10-12037-2010, 2010.
- Hönninger, G.: Halogen Oxide Studies in the Boundary Layer by Multi Axis Differential Optical Absorption Spectroscopy and Active Longpath-DOAS, PhD, University of Heidelberg, 2002.
- Huff, A. K. and Abbatt, J. P. D.: Kinetics and product yields in the heterogeneous reactions of HOBr with ice surfaces containing NaBr and NaCl, *J. Phys. Chem. A*, 106, 5279–5287, 2002.
- Jacob, D. J.: Heterogeneous chemistry and tropospheric ozone, *Atmos. Environ.*, 34, 2131–2159, 2000.
- Jobson, B., Niki, H., Yokouchi, Y., Bottenheim, J., Hopper, F., and Leaitch, R.: Measurements of C₂–C₆ hydrocarbons during the Polar Sunrise 1992 Experiment: Evidence for Cl atom and Br atom chemistry, *J. Geophys. Res.*, 99, 25355–25368, 1994.
- Kukui, A., Kirchner, U., Benter, T., and Schindler, R. N.: A gas kinetic investigation of HOBr reactions with Cl(²P), O(³P) and OH(²II). The reaction of BrCl with OH(²II), *Ber. Bunsen. Phys. Chem.*, 100, 455–461, 1996.
- Kuo, K. K.: Principles of combustion, John Wiley & Sons, New York, 1986.
- Lancaster, D. G., Fried, A., Wert, B., Henry, B., and Tittel, F. K.: Difference-frequency-based tunable absorption spectrometer for detection of atmospheric formaldehyde, *Appl. Optics*, 39, 24, 4436–4443, doi:10.1364/AO.39.004436, 2000.
- Lary, D.: Gas phase atmospheric bromine photochemistry, *J. Geophys. Res.*, 101, 1505–1516, 1996.
- Le Bras, G. and Platt, U.: A possible mechanism for combined chlorine and bromine catalyzed destruction of tropospheric ozone in the Arctic, *Geophys. Res. Lett.*, 22, 599–602, 1995.
- Lehrer, E., Hönninger, G., and Platt, U.: A one dimensional model study of the mechanism of halogen liberation and vertical transport in the polar troposphere, *Atmos. Chem. Phys.*, 4, 2427–2440, doi:10.5194/acp-4-2427-2004, 2004.
- Liao, J., Sihler, H., Huey, L. G., Neuman, J. A., Tanner, D. J., Friess, U., Platt, U., Flocke, F. M., Orlando, J. J., Shepson, P. B., Beine, H. J., Weinheimer, A. J., Sjostedt, S. J., Nowak, J. B., Knapp, D. J., Staebler, R. M., Zheng, W., Sander, R., Hall, S. R., and Ullmann, K.: A comparison of Arctic BrO measurements by chemical ionization mass spectrometry and long path-differential optical absorption spectroscopy, *J. Geophys. Res.*, 116, D14, doi:10.1029/2010JD014788, 2011.
- Liao, J., Huey, L. G., Scheuer, E., Dibb, J. E., Stickel, R. E., Tanner, D. J., Neuman, J. A., Nowak, J. B., Choi, S., Wang, Y., Salawitch, R. J., Carty, T., Chance, K., Kurosu, T., Suleiman, R., Weinheimer, A. J., Shetter, R. E., Fried, A., Brune, W., Anderson, B., Zhang, X., Chen, G., Crawford, J., Hecobian, A., and Ingall, E. D.: Characterization of soluble bromide measurements and a case study of BrO observations during ARCTAS, *Atmos. Chem. Phys.*, 12, 1327–1338, doi:10.5194/acp-12-1327-2012, 2012a.
- Liao, J., Huey, L., Tanner, D., Flocke, F., Orlando, J., Neuman, J., Nowak, J., Weinheimer, A., Hall, S., Smith, J., Fried, A., Staebler, R., Wang, Y., Koo, J.-H., Cantrell, C., Weibring, P., Walega, J., Knapp, D., Shepson, P., and Stephens, C.: Observations of inorganic bromine (HOBr, BrO, and Br₂) speciation at Barrow, Alaska, in spring 2009, *J. Geophys. Res.*, 117, D00R16, doi:10.1029/2011JD016641, 2012b.
- Liao, J., Huey, L. G., Liu, Z., Tanner, D. J., Cantrell, C. A., Orlando, J. J., Flocke, F. M., Shepson, P. B., Weinheimer, A. J., Hall, S. R., Beine, H. J., Wang, Y., Ingall, E. D., Stephens, C. R., Hornbrook, R. S., Apel, E., Fried, A., Mauldin, L., Smith, J. N., Staebler, R. M., Neuman, J. A., and Nowak, J. B.: High levels of molecular chlorine in the Arctic atmosphere, *Nat. Geosci.*, 7, 91–94, doi:10.1038/ngeo2046, 2014.
- Mahajan, A., Shaw, M., Oetjen, H., Hornsby, K., Carpenter, L., Kaleschke, L., Tian-Kunze, X., Lee, J., Moller, S., and Edwards, P.: Evidence of reactive iodine chemistry in the Arctic boundary layer, *J. Geophys. Res.*, 115, D20303, doi:10.1029/2009JD013665, 2010.
- Mallard, W. G., Westley, F., Herron, J. T., Hampson, R. F., and Frizzel, D. H.: NIST Chemical Kinetics Database: Version 5.0 National Institute of Standards and Technology, Gaithersburg, MD, 1993.
- Martinez, M., Arnold, T., and Perner, D.: The role of bromine and chlorine chemistry for arctic ozone depletion events in Ny-

- Ålesund and comparison with model calculations, *Ann. Geophys.*, 17, 941–956, doi:10.1007/s00585-999-0941-4, 1999.
- McFiggans, G., Plane, J. M. C., Allan, B. J., Carpenter, L. J., Coe, H., and O'Dowd, C.: A modeling study of iodine chemistry in the marine boundary layer, *J. Geophys. Res.*, 105, 14371–14385, 2000.
- McFiggans, G., Cox, R. A., Mössinger, J. C., Allan, B. J., and Plane, J. M. C.: Active chlorine release from marine aerosols: Roles for reactive iodine and nitrogen species, *J. Geophys. Res.*, 107, ACH 10-1–ACH 10-13, doi:10.1029/2001JD000383, 2002.
- Michalowski, B. A., Francisco, J. S., Li, S. M., Barrie, L. A., Bottenheim, J. W., and Shepson, P. B.: A computer model study of multiphase chemistry in the Arctic boundary layer during polar sunrise, *J. Geophys. Res.*, 105, 15131–15145, 2000.
- Mielke, L. H., Furgeson, A., and Osthoff, H. D.: Observation of ClNO₂ in a mid-continental urban environment, *Environ. Sci. Technol.*, 45, 8889–8896, 2011.
- Monks, P. S.: Gas-phase radical chemistry in the troposphere, *Chem. Soc. Rev.*, 34, 376–395, 2005.
- Neuman, J. A., Nowak, J. B., Huey, L. G., Burkholder, J. B., Dibb, J. E., Holloway, J. S., Liao, J., Peischl, J., Roberts, J. M., Ryerson, T. B., Scheuer, E., Stark, H., Stickel, R. E., Tanner, D. J., and Weinheimer, A.: Bromine measurements in ozone depleted air over the Arctic Ocean, *Atmos. Chem. Phys.*, 10, 6503–6514, doi:10.5194/acp-10-6503-2010, 2010.
- Orlando, J. J. and Tyndall, G. S.: Rate Coefficients for the Thermal Decomposition of BrONO₂ and the Heat of Formation of BrONO₂, *J. Phys. Chem.*, 100, 19398–19405, doi:10.1021/jp9620274, 1996.
- Oum, K., Lakin, M., and Finlayson-Pitts, B.: Bromine activation in the troposphere by the dark reaction of O₃ with seawater ice, *Geophys. Res. Lett.*, 25, 3923–3926, 1998b.
- Papanastasiou, D. K., McKeen, S. A., and Burkholder, J. B.: The very short-lived ozone depleting substance CHBr₃ (bromoform): revised UV absorption spectrum, atmospheric lifetime and ozone depletion potential, *Atmos. Chem. Phys.*, 14, 3017–3025, doi:10.5194/acp-14-3017-2014, 2014.
- Piot, M. and von Glasow, R.: The potential importance of frost flowers, recycling on snow, and open leads for ozone depletion events, *Atmos. Chem. Phys.*, 8, 2437–2467, doi:10.5194/acp-8-2437-2008, 2008.
- Platt, U. and Janssen, C.: Observation and role of the free radicals NO₃, ClO, BrO and IO in the troposphere, *Faraday Discuss.*, 100, 175–198, 1995.
- Pöhler, D., Vogel, L., Frieß, U., and Platt, U.: Observation of halogen species in the Amundsen Gulf, Arctic, by active long-path differential optical absorption spectroscopy, *P. Natl. Acad. Sci. USA*, 107, 6582–6587, doi:10.1073/pnas.0912231107, 2010.
- Pratt, K. A., Custard, K. D., Shepson, P. B., Douglas, T. A., Pöhler, D., General, S., Zielcke, J., Simpson, W. R., Platt, U., Tanner, D. J., Huey, L. G., Carlsen, M., and Stirn, B. H.: Photochemical production of molecular bromine in Arctic surface snowpacks, *Nat. Geosci.*, 6, 351–356, doi:10.1038/ngeo1779, 2013.
- Raso, A. R. W., Custard, K. D., Pratt, K. A., Tanner, D. J., Huey, L. G., and Shepson, P. B.: Active molecular iodine snowpack photochemistry in the Arctic, *P. Natl. Acad. Sci. USA*, in review, 2017.
- Ridley, B., Grahek F., and Walega, J.: A small high-sensitivity, medium-response ozone detector suitable for measurements from light aircraft, *J. Atmos. Oceanic Technol.*, 9, 142–148, 1992.
- Russo, R., Zhou, Y., White, M., Mao, H., Talbot, R., and Sive, B.: Multi-year (2004–2008) record of nonmethane hydrocarbons and halocarbons in New England: Seasonal variations and regional sources, *Atmos. Chem. Phys.*, 10, 4909–4929, doi:10.5194/acp-10-4909-2010, 2010.
- Ryerson, T. B., Williams, E. J., and Fehsenfeld, F. C.: An efficient photolysis system for fast-response NO₂ measurements, *J. Geophys. Res.*, 105, 26447–26461, doi:10.1029/2000JD900389, 2000.
- Saiz-Lopez, A., Plane, J. M. C., Mahajan, A. S., Anderson, P. S., Bauguitte, S. J.-B., Jones, A. E., Roscoe, H. K., Salmon, R. A., Bloss, W. J., Lee, J. D., and Heard, D. E.: On the vertical distribution of boundary layer halogens over coastal Antarctica: implications for O₃, HO_x, NO_x and the Hg lifetime, *Atmos. Chem. Phys.*, 8, 887–900, doi:10.5194/acp-8-887-2008, 2008.
- Sander, R., Vogt, R., Harris, G. W., and Crutzen, P. J.: Modelling the chemistry of ozone, halogen compounds, and hydrocarbons in the arctic troposphere during spring, *Tellus B*, 49, 522–532, 1997.
- Sander, R., Keene, W. C., Pszenny, A. A. P., Arimoto, R., Ayers, G. P., Baboukas, E., Caine, J. M., Crutzen, P. J., Duce, R. A., Hönninger, G., Huebert, B. J., Maenhaut, W., Mihalopoulos, N., Turekian, V. C., and Van Dingenen, R.: Inorganic bromine in the marine boundary layer: a critical review, *Atmos. Chem. Phys.*, 3, 1301–1336, doi:10.5194/acp-3-1301-2003, 2003.
- Sander, S. P., Golden, D., Kurylo, M., Moortgat, G., Wine, P., Ravishankara, A., Kolb, C., Molina, M., Finlayson-Pitts, B., and Huie, R.: Chemical kinetics and photochemical data for use in atmospheric studies evaluation number 15, <http://hdl.handle.net/2014/41648>, 2006.
- Shetter, R. E. and Müller, M.: Photolysis frequency measurements using actinic flux spectroradiometry during the PEM-Tropics mission: Instrumentation description and some results, *J. Geophys. Res.*, 104, 5647–5661, 1999.
- Shepson, P. B., Sirju, A.-P., Hopper, J. F., Barrie, L. A., Young, V., Niki, H., and Dryfhout, H.: Sources and sinks of carbonyl compounds in the Arctic Ocean boundary layer: a polar ice floe experiment, *J. Geophys. Res.*, 101, 21081–21089, 1996.
- Staebler, R. M., den Hartog, G., Georgi, B., and Sterdiek, T. D.: Aerosol size distribution in Arctic haze during the Polar Sunrise Experiment 1992, *J. Geophys. Res.*, 99, 25429–25437, 1994.
- Sumner, A. L., and Shepson, P. B.: Snowpack production of formaldehyde and its effect on the Arctic troposphere, *Nature*, 398, 230–233, 1999.
- Stephens, C. R., Shepson, P. B., Steffen, A., Bottenheim, J. W., Liao, J., Huey, L. G., Apel, E., Weinheimer, A., Hall, S. R., and Cantrell, C.: The relative importance of chlorine and bromine radicals in the oxidation of atmospheric mercury at Barrow, Alaska, *J. Geophys. Res.*, 117, D00R11, doi:10.1029/2011JD016649, 2012.
- Sturges, W. and Barrie, L.: Chlorine, bromine and iodine in Arctic aerosols, *Atmos. Environ.*, 22, 1179–1194, 1988.
- Tang, T. and McConnell, J.: Autocatalytic release of bromine from Arctic snow pack during polar sunrise, *Geophys. Res. Lett.*, 23, 2633–2636, 1996.
- Thomas, J. L., Stutz, J., Lefer, B., Huey, L. G., Toyota, K., Dibb, J. E., and von Glasow, R.: Modeling chemistry in and above snow

- at Summit, Greenland – Part 1: Model description and results, *Atmos. Chem. Phys.*, 11, 4899–4914, doi:10.5194/acp-11-4899-2011, 2011.
- Thompson, C. R., Shepson, P. B., Liao, J., Huey, L. G., Apel, E. C., Cantrell, C. A., Flocke, F., Orlando, J., Fried, A., Hall, S. R., Hornbrook, R. S., Knapp, D. J., Mauldin III, R. L., Montzka, D. D., Sive, B. C., Ullmann, K., Weibring, P., and Weinheimer, A.: Interactions of bromine, chlorine, and iodine photochemistry during ozone depletions in Barrow, Alaska, *Atmos. Chem. Phys.*, 15, 9651–9679, doi:10.5194/acp-15-9651-2015, 2015.
- Thornton, J. A., Kercher, J. P., Riedel, T. P., Wagner, N. L., Cozic, J., Holloway, J. S., Dubé, W. P., Wolfe, G. M., Quinn, P. K., Middlebrook, A. M., Alexander, B., and Brown, S. S.: A large atomic chlorine source inferred from mid-continental reactive nitrogen chemistry, *Nature*, 464, 271–274, 2010.
- Toyota, K., McConnell, J. C., Lupu, A., Neary, L., McLinden, C. A., Richter, A., Kwok, R., Semeniuk, K., Kaminski, J. W., Gong, S.-L., Jarosz, J., Chipperfield, M. P., and Sioris, C. E.: Analysis of reactive bromine production and ozone depletion in the Arctic boundary layer using 3-D simulations with GEM-AQ: inference from synoptic-scale patterns, *Atmos. Chem. Phys.*, 11, 3949–3979, doi:10.5194/acp-11-3949-2011, 2011.
- Toyota, K., McConnell, J. C., Staebler, R. M., and Dastoor, A. P.: Air–snowpack exchange of bromine, ozone and mercury in the springtime Arctic simulated by the 1-D model PHANTAS – Part 1: In-snow bromine activation and its impact on ozone, *Atmos. Chem. Phys.*, 14, 4101–4133, doi:10.5194/acp-14-4101-2014, 2014.
- Troy, R. C., Kelley, M. D., Nagy, J. C., and Margerum, D. W.: Non-metal redox kinetics: Iodine monobromide reaction with iodide ion and the hydrolysis of IBr, *Inorg. Chem.*, 30, 4838–4845, 1991.
- Vogt, R., Crutzen, P. J., and Sander, R.: A mechanism for halogen release from sea-salt aerosol in the remote marine boundary layer, *Nature*, 383, 327–330, doi:10.1038/383327a0, 1996.
- Wallington, T. J., Skewes, L. M., Siegl, W. O., and Japar, S. M.: A relative rate study of the reaction of bromine atoms with a variety of organic compounds at 295 K, *Int. J. Chem. Kinet.*, 21, 1069–1076, 1989.
- Wang, T. X., Kelley, M. D., Cooper, J. N., Beckwith, R. C., and Margerum, D. W.: Equilibrium, kinetic, and UV-spectral characteristics of aqueous bromine chloride, bromine, and chlorine species, *Inorg. Chem.*, 33, 5872–5878, 1994.
- Wennberg, P., Hanisco, T., Jaegle, L., Jacob, D., Hints, E., Lanzendorf, E., Anderson, J., Gao, R. S., Keim, E., and Donnelly, S.: Hydrogen radicals, nitrogen radicals, and the production of O₃ in the upper troposphere, *Science*, 279, 49–53, 1998.
- Young, C. J., Washenfelder, R. A., Roberts, J. M., Mielke, L. H., Osthoff, H. D., Tsai, C., Pikelnyai, O., Stutz, J., Veres, P. R., Cochran, A. K., VandenBoer, T. C., Flynn, J., Grossberg, N., Haman, C. L., Lefer, B., Stark, H., Graus, M., de Gouw, J., Gilman, J. B., Kuster, W. C., and Brown, S. S.: Vertically resolved measurements of nighttime radical reservoirs in Los Angeles and their contribution to the urban radical budget, *Environ. Sci. Technol.*, 46, 10965–10973, 2012.
- Zeng, T., Wang, Y., Chance, K., Blake, N., Blake, D., and Ridley, B.: Halogen-driven low-altitude O₃ and hydrocarbon losses in spring at northern high latitudes, *J. Geophys. Res.*, 111, D17313, doi:10.1029/2005JD006706, 2006.